Thoracic Aortic Aneurysms, Fistula, and Thrombus

Maria Cristina Firetto, Marcello Petrini, Francesco Sala, Maurizio Domanin, Giovanni Terribile, and Pietro Raimondo Biondetti

Contents

M.C. Firetto, MD (✉) • M. Domanin, MD
G. Terribile • P.R. Biondetti, MD
Fondazione IRCCS Ca' Granda,
Ospedale Maggiore Policlinico, Milan, Italy
e-mail: firettomariacristina@gmail.com

M. Petrini, MD
Università degli Studi di Milano, Postgraduation School in Radiodiagnostics, Milan, Italy

F. Sala, MD
Department of Radiology, A.O. Papa Giovanni XXIII, Bergamo, Italy

Abstract

Thoracic aortic aneurysms (TAAs) are abnormal dilatation occurring in the thoracic aorta. They can be classified according to location, morphology, and etiology. TAAs can be divided into true aneurysms and false aneurysms (also called pseudoaneurysms). True aneurysms are usually associated with fusiform dilatation of the aorta and most commonly due to atherosclerosis. False aneurysms are typically saccular with a narrow neck and most commonly due to trauma, penetrating atherosclerotic ulcers, or infections (mycotic aneurysm). Atherosclerosis, genetic causes, aortitis, trauma, and dissection can be the causes of TAAs. MDCT allows the evaluation of TAAs in terms of morphologic features, extent, and signs of instability or impending rupture. Acute aortic thrombosis and aortic fistula with esophagus or bronchi are rare but life-threatening complications of aortic disease. Imaging findings may be subtle.

Med Radiol Diagn Imaging (2016)
DOI 10.1007/174_2016_44, © Springer International Publishing Switzerland

1 Thoracic Aortic Aneurysms

1.1 Definition

Aneurysm etymologically derives from the Greek "aneurysma," i.e., "dilation," and it is defined as a permanent dilatation of an artery having a ≥50 % increase in diameter compared with its expected normal diameter. Aneurysmal degenerations occurring in the thoracic aorta are defined as thoracic aortic aneurysms (TAAs). TAAs can be classified according to location, morphology, and etiology. While in the real aortic aneurysms all three layers (intima, media, and adventitia) of the aortic wall are present in the aneurysmal wall, in pseudoaneurysms one or more of these layers are absent due to the lesion that originates from them, for example, trauma or penetrating atherosclerotic aortic ulcers.

1.2 Location

The thoracic aorta consists of the aortic root, ascending aorta, aortic arch, and descending thoracic aorta (Agarwal et al. 2009). The aortic root consists of the annulus, sinuses of Valsalva, and sinotubular junction. The annulus, a fibrous band surrounding the aorta, is located at the aortoventricular junction. The Valsalva sinus is a dilatation of the aortic root just above the aortic valve. At its upper level, at sinotubular junction, the Valsalva sinus becomes the tubular ascending aorta. The ascending aorta extends from the root to the origin of the right brachiocephalic artery (also called innominate artery); the arch, from the right brachiocephalic artery to the attachment of the ligamentum arteriosum; and the descending aorta, from the ligamentum arteriosum to the aortic hiatus in the diaphragm (Lodi et al. 2004). The arch may be subdivided into proximal (right brachiocephalic artery to left subclavian artery) and distal (left subclavian artery to attachment of the ligamentum arteriosum) segments (Mukherjee and Rajagopalan 2007). The distal arch, also referred to as the isthmus, may be narrower than the proximal descending aorta (Mukherjee and Rajagopalan 2007).

A TAA is defined as a permanent abnormal dilatation of the thoracic aorta (Green and Klein 2007). Although the aortic diameter increases with age, the normal diameter of the midascending aorta should always be less than 4 cm, and that of the descending aorta no more than 3 cm (Aronberg et al. 1984).

TAAs may involve one or more aortic segments (Goldstein et al. 2015): 60 % of TAAs involve the aortic root and/or ascending tubular aorta, 40 % the descending aorta, 10 % the arch, and 10 % the thoracoabdominal aorta (Isselbacher 2005).

1.3 Morphology and Pathophysiology

1.3.1 Morphology

An arterial blood vessel has the following three layers: intima (a thin inner layer made of endothelial cells, easily traumatized), media (a thick middle layer, composed of smooth muscle cells and multiple layers of elastic laminae that provide tensile strength, distensibility, and elasticity), and adventitia (a rather thin outer layer, made of collagen and vasa vasorum). The wall of a *true aneurysm* (Fig. 1a, b) involves all three layers, and the aneurysm is contained inside the endothelium. It is usually associated with fusiform dilatation of the aorta and is most commonly due to atherosclerosis (Posniak et al. 1990). The wall of a *false or pseudoaneurysm* involves only the outer layer, and it is contained by the adventitia or periadventitial tissues. It is typically saccular (Fig. 2a–e) with a narrow neck, and it is most commonly due to trauma, penetrating atherosclerotic ulcers, or infections (mycotic aneurysm) (Lesko et al. 1997). There are also various morphologic shapes of the aortic root and ascending aorta, some of which suggest specific etiologies. For example, *annuloaortic ectasia*, a condition characterized by dilated sinuses of Valsalva with effacement of the sinotubular junction producing a pear-shaped aorta that tapers to a normal aortic arch, is most commonly associated with Marfan syndrome (Fig. 3a, b).

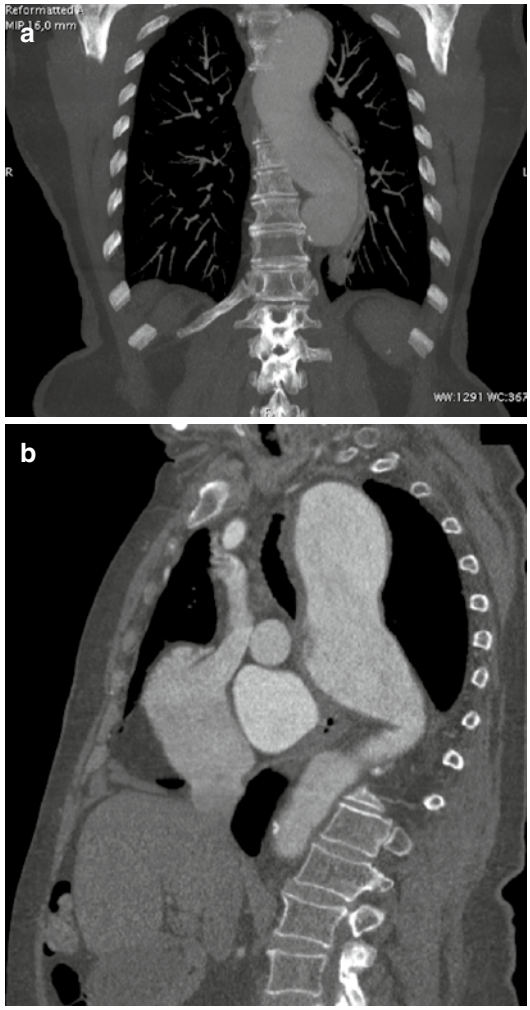

Fig. 1 Thoracic aortic aneurysm in a 59-year-old man. Contrast-enhanced coronal MIP image (**a**) and sagittal MPR image (**b**) show a true aneurysm, with fusiform dilatation of the descending aorta

1.3.2 Pathophysiology

The pathogenesis of aneurysm is extremely complex and not completely understood; most likely, aneurysms result from the interaction of multiple factors, systemic and local hemodynamic features (Michel et al. 2011). The elastic properties of the aorta are important for its normal function. The elasticity of the wall allows the aorta to accept the pulsatile output of the left ventricle in systole and to modulate continued forward flow during diastole. With aging, the medial elastic fibers become thinned and fragmented, with the increase in collagen and ground substance. Elasticity and compliance of the aortic wall are progressively lost, with the increase in pulse pressure and with progressive dilatation of the aorta (Goldstein et al. 2015). Many authors suggest that a group of enzymes called matrix metalloproteinases (MMPs) plays a significant role in the destruction of extracellular matrix in the aortic wall. MMPs lead to the degradation of these structural proteins with elastic fiber fragmentation and loss and degeneration of the tunica media with loss of elasticity and weakening of the aortic wall and consequent dilation (Sakalihasan et al. 2005). Hemodynamic factors probably play a fundamental role in the formation of aortic aneurysms. The human aorta is a relatively low-resistance circuit for circulating blood while the lower extremities have higher arterial resistance (Hoshina et al. 2003). Repeated hydrostatic trauma may injure a diseased aortic wall and contribute to aneurysmal development. In case of concomitant systemic hypertension, it can accelerate the expansion of known aneurysms and may contribute to their initial formation (Piccinelli et al. 2013). Wall rupture follows the basic principles of material failure, i.e., an aneurysm breaks open when mural stress or deformation meets an appropriate failure criterion. The law of Laplace states that wall tension is proportional to the pressure and to the radius of the arterial conduit ($T = P \times R$). As diameter increases, wall tension increases, which contributes to increasing diameter and risk of rupture. Also increased pressure and aneurysm size aggravate wall tension and therefore increase the risk of rupture. The use of the law of Laplace to predict AAA rupture potential is erroneous, because the AAA wall geometry is not a simple cylinder or sphere with a single radius of curvature, and wall stress alone is not sufficient to predict AAA rupture. So AAA diameter cannot be considered as the only determinant factor of either wall strength or wall stress (Piccinelli et al. 2013). Various indices have been proposed to create a more reliable and patient-specific criteria for clinical practice. Despite many progresses, the majority of the proposed criteria for risk stratification and decision making still rely on

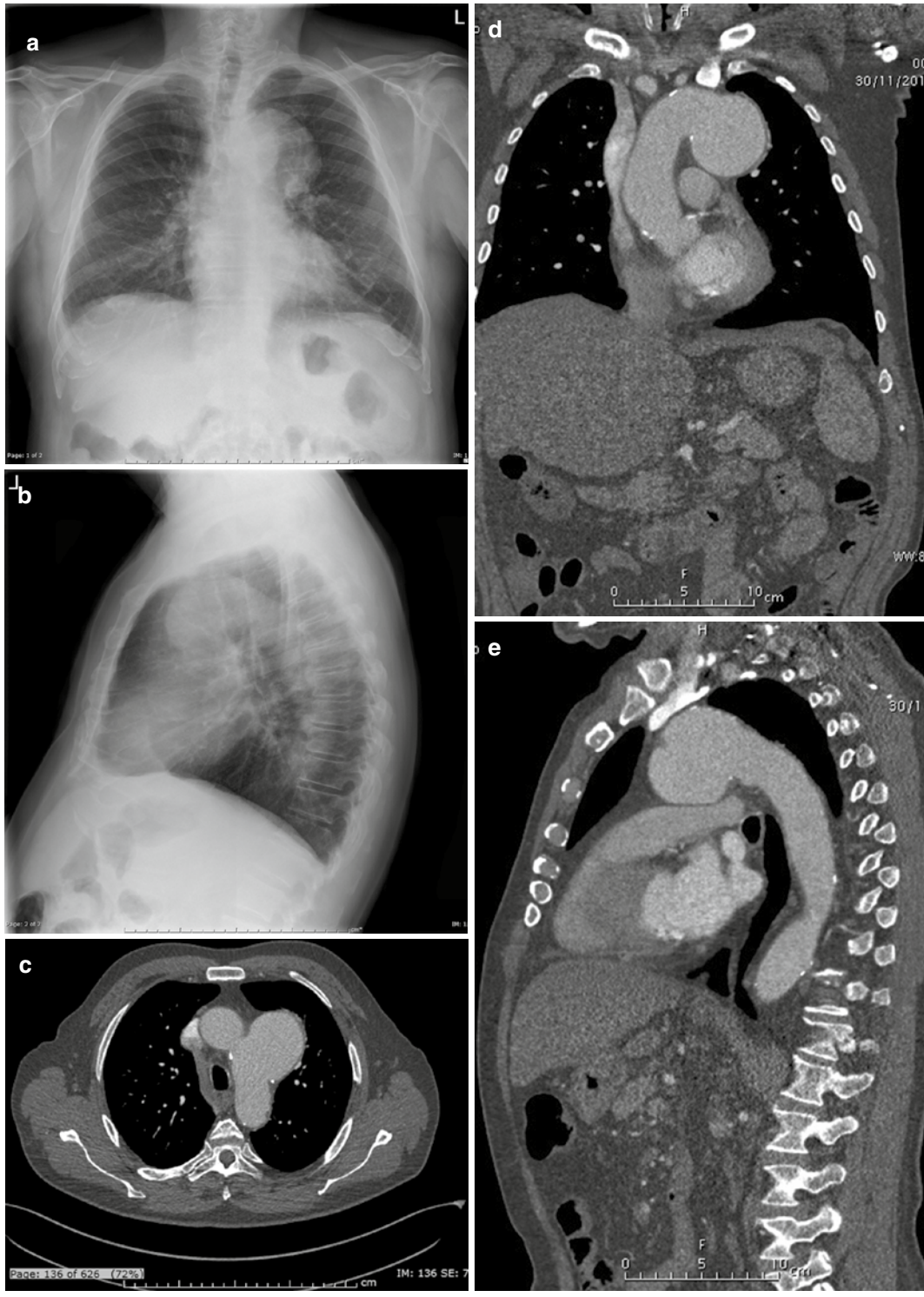

Fig. 2 PA and lateral X-rays (**a**, **b**) show widened mediastinum, opacification of the aortopulmonary window, and rightward deviation of the trachea. Axial (**c**), coronal (**d**), and sagittal (**e**) MPR CT images show saccular dilatation of the proximal descending aorta

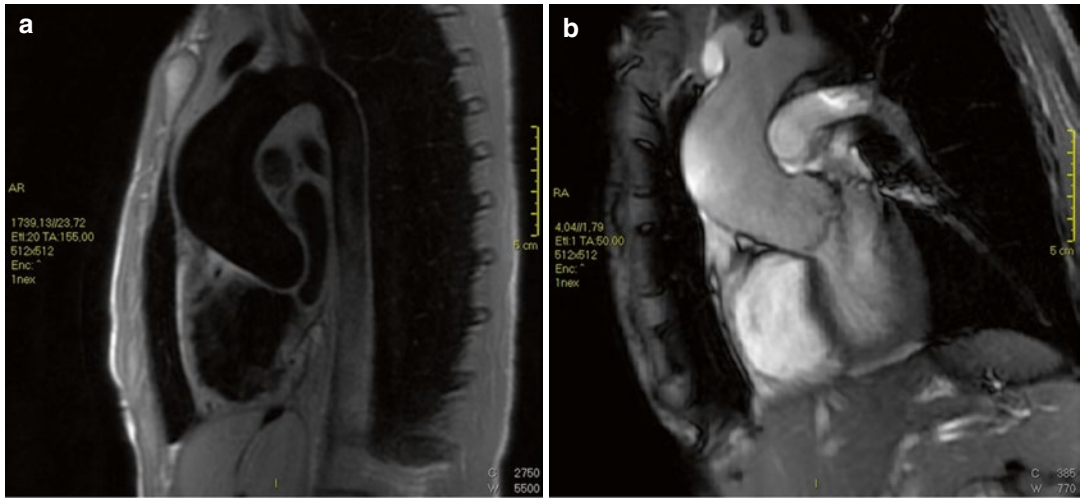

Fig. 3 Marfan syndrome and annuloaortic ectasia in a 42-year-old woman. (**a**) T1-weighted and (**b**) gradient echo sagittal oblique MRI show a pear-shaped aorta that tapers to a normal aortic arch, a characteristic finding in Marfan syndrome

empirical measurements rather than on the analysis of biomechanical properties (Creasy et al. 1997); among these are maximum AAA diameter (Greenhalgh 2004), currently the prevalent index for the evaluation of risk of rupture; AAA expansion rate (Hirose and Takamiya 1998); wall stiffness (Fillinger et al. 2003); intraluminal thrombus thickness (Speelman et al. 2010); and AAA wall peak stress (Raghavan et al. 2000; McGloughlin and Doyle 2010). The presence of anisotropic displacement of the AAA lumen boundary and their link to hemodynamic forces have been assessed, highlighting a new possible role for hemodynamics in the study of AAA progression (Piccinelli et al. 2013).

1.4 Etiology

Atherosclerosis is the cause of approximately 70 % of all TAAs (Lesko et al. 1997) and contributes to the formation of aortic aneurysms secondary to the degeneration of the components of the aortic wall. Atherosclerotic aneurysms are the most common type; usually they are seen in the elderly and typically characterized by intimal calcification and fibrous plaques along the aorta. The majority of them are fusiform, up to 20 % may be saccular (Posniak et al. 1990), and they occur in the descending thoracic aorta and rarely involve only the ascending aorta (Lesko et al. 1997) (Fig. 4a, b).

Because an abdominal aortic aneurysm occurs in 28 % of patients with TAA, initial CT evaluation may include the entire thoracoabdominal aorta (Bickerstaff et al. 1982).

Many authors consider *genetic causes* as a leading factors in the formation and development of aortic aneurysms. Inherited disorders of connective tissue contribute to the formation of aortic aneurysms. *Marfan syndrome* is a multisystemic connective tissue, autosomal dominant inherited disorder (Goldstein et al. 2015). One of the hallmark features is dilatation or dissection of the aortic root (Daimon et al. 2008). Aortic aneurysms without annuloaortic ectasia are also common. Annuloaortic ectasia, especially with dilatation of the aortic root, is found in 60–80 % of adults with Marfan syndrome. It usually begins with dilatation of the aortic sinuses, which progresses first into the sinotubular junction, than into the aortic annulus. Dilatation of the aortic root causes aortic valve insufficiency that may progress to aortic root dissection or rupture (Vasan et al. 1995). The aortic aneurysms rarely show intimal calcification or atherosclerotic thrombosis; they occur

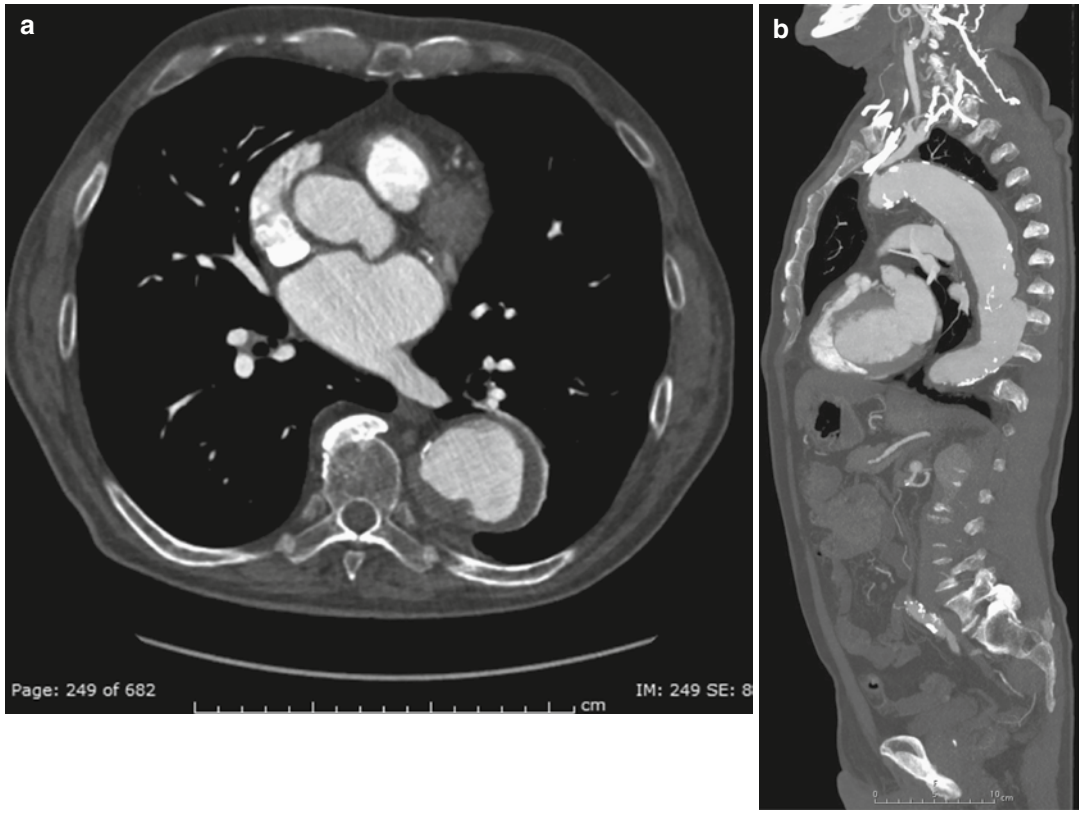

Fig. 4 Descending TAA in an 82-year-old man. Contrast-enhanced (**a**) axial CT image shows an atherosclerotic aorta, with fusiform aneurysm. (**b**) Sagittal MIP image shows the overall extent of the aneurysm in the descending aorta

commonly and develop more rapidly in younger patients. After the initial diagnosis of aortopathy by TTE, CT or MRI is recommended to confirm the size of the aorta and to document the diameters of the distal ascending aorta, aortic arch, and descending aortic segments. Repeated CT or MRI, about every 3 years, is recommended to reassess the aortic arch and the descending aorta. Prophylactic surgery for annuloaortic ectasia is recommended when the diameter of the Valsalva sinus exceeds 5.5 cm in an adult and 5.0 cm in a child, when the diameter of the Valsalva sinus is less than 5.0 cm but in a rapid rate of aortic aneurysm expansion (increase in dilatation by more than 1 cm per year), or when there is a family history of aortic dissection (Wolak et al. 2008; Kälsch et al. 2013; De Backer et al. 2006). Composite surgical replacement of the aortic root and valve is commonly performed with or without coronary reimplantation (Fig. 5a, b).

Other genetic conditions associated with aortic dilatation are bicuspid valve-related aortopathy (BAV), Loeys–Dietz syndrome, Turner syndrome, familial TAA, and Ehlers–Danlos syndrome. *Ehlers–Danlos syndrome* (EDS) is an autosomal dominant disorder with vascular involvement (arterial dilatation and rupture). The imaging characteristics of aortic aneurysms in Ehlers–Danlos syndrome resemble those in Marfan syndrome.

Aortitis is a general term that refers to a broad category of infectious or noninfectious conditions, in which there is abnormal inflammation of the aortic wall. These inflammatory conditions have different clinical and morphologic features and variable prognoses (Restrepo et al. 2011). The differentiation between infectious (mycotic) and noninfectious aneurysms is important because, as mycotic aneurysms are treated with antibiotic therapy and surgical debridement with

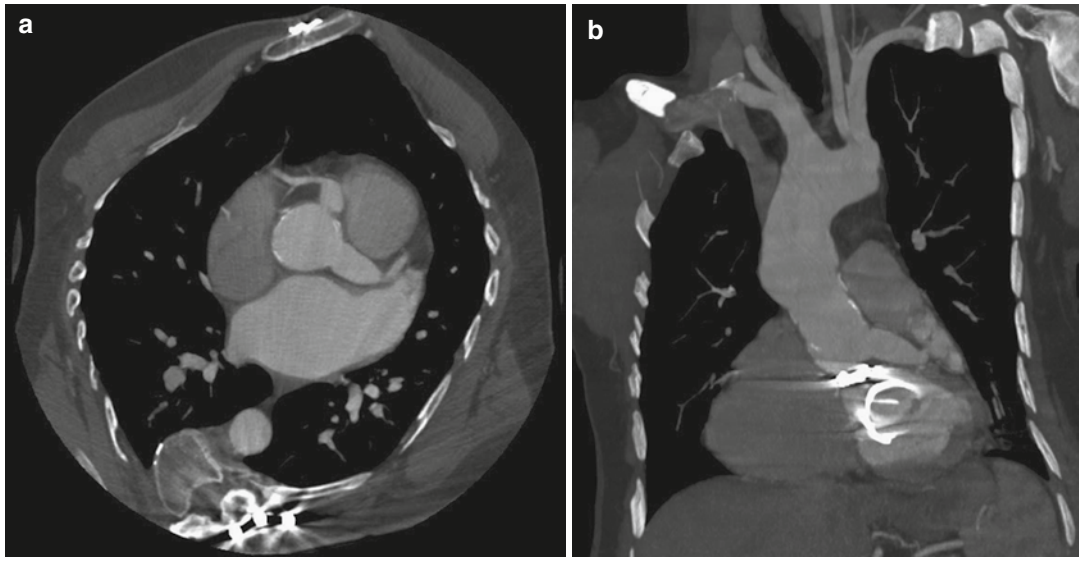

Fig. 5 Axial–oblique (**a**) and coronal–oblique MIP (**b**) CT sections at the level of the coronary artery origin, after ascending aorta replacement with graft. Note the persistent dilation of both proximal left and right coronary arteries

or without surgical revascularization, noninfectious aneurysms are managed by steroids and immunosuppressive drugs (Nagpal et al. 2015).

Noninfectious aortitis may be part of a systemic disorder (Gornik and Creager 2008). The association between rheumatic diseases and aortic involvement is well known, but the prevalence of aortic involvement in the different rheumatic diseases is quite variable. Rheumatic diseases (Slobodin et al. 2006) with a high prevalence (>10 %) of aortic involvement include Takayasu arteritis (Fig. 6a–c), giant cell arteritis (GCA), long-standing ankylosing spondylitis, Cogan syndrome (interstitial keratitis, iritis, conjunctival or subconjunctival hemorrhage, fever, aortic insufficiency) (Fig. 7a, b), and relapsing polychondritis. Rheumatic diseases in which aortic involvement is an uncommon well-documented complication include rheumatoid arthritis, seronegative spondyloarthropathies, Behçet disease, and systemic lupus erythematosus (SLE). Aortitis most commonly affects the ascending aorta in rheumatoid arthritis (Fig. 8a, b), ankylosing spondylitis, giant cell arteritis, and relapsing polychondritis (Posniak et al. 1990). These conditions may also be associated with aortic valve insufficiency. Aortitis in rheumatic fever can be segmental, limited to the ascending aorta, or it can involve the abdominal aorta or the entire aorta (Lande and Berkmen 1976; Posniak et al. 1990). Takayasu arteritis commonly affects the aortic arch and its major branches, with variable involvement of the abdominal aorta and pulmonary arteries; although Takayasu arteritis typically causes arterial stenosis and occlusion, aneurysms may also occur. Inflammatory aneurysms differ from atherosclerotic aneurysms because of the presence of dense perianeurysmal fibrosis and thickened aortic wall (Restrepo et al. 2011). The prevalence is 5–25 % of all abdominal aortic aneurysms. Inflammatory aneurysms of the ascending aorta and aortic arch are much less frequent, usually associated with concomitant inflammatory aneurysms in the abdominal aorta (Girardi and Coselli 1997). CT shows a hypoattenuating mass with periaortic wall thickening that spares the posterior wall. After intravenous administration of contrast material, rapid luminal opacification is followed by delayed enhancement of the soft-tissue component.

Infected (*mycotic*) *aneurysms*. Infectious aortitis is secondary to gram-positive bacteria such as the *Staphylococcal* species, *Enterococcus* species, and *Streptococcus pneumonia*, responsible

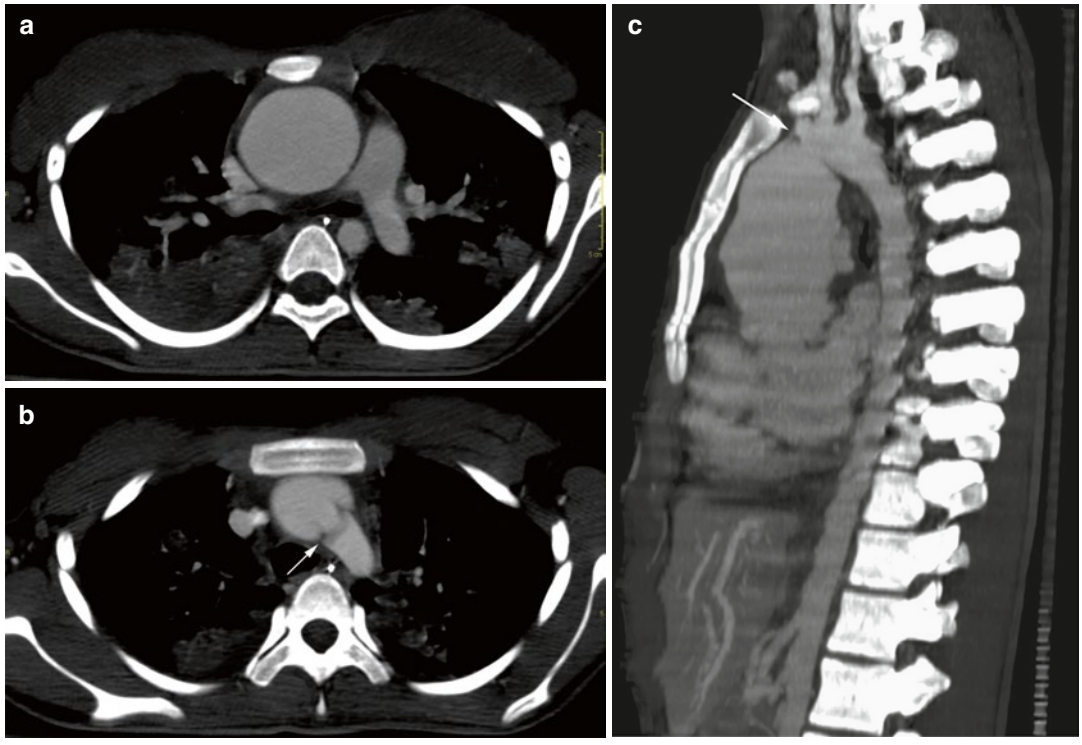

Fig. 6 Axial (**a**, **b**) and sagittal (**c**) CT MIP images in a patient with Takayasu arteritis. Fusiform aneurysm of the ascending aorta (**a**, **c**) and atypical coarctation at the level of the aortic arch (*arrows* in **b**, **c**) are well demonstrated

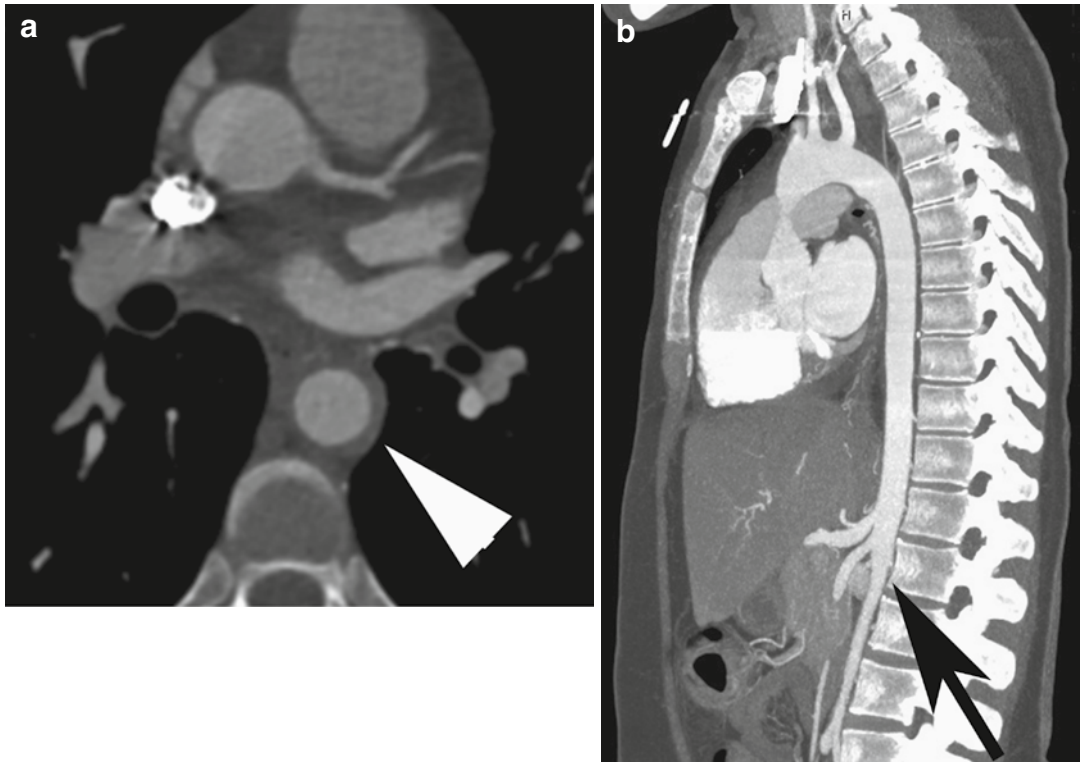

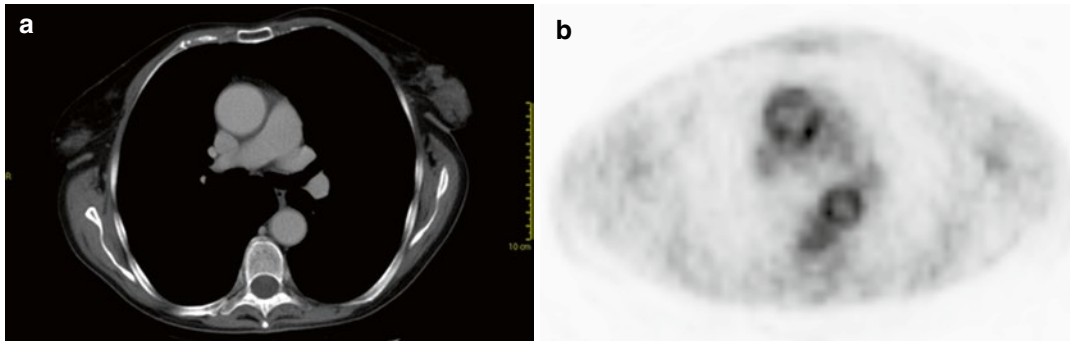

Fig. 8 Axial CT (**a**) and PET (**b**) images of a patient with rheumatoid arteritis. There is questionable wall thickening of the normal caliber thoracic aorta at CT (**a**). PET shows abnormal uptake of the aortic wall due to the inflammatory changes

of 60 % of the infections. Gram-negative bacilli (*Salmonella* species in the majority of cases) are also a frequent cause of aortic infection; however, they are more prevalent in infectious abdominal aortitis (Revest et al. 2007). Aortic infection by *Mycobacterium tuberculosis*, an uncommon problem in developed countries, may occur as a result of the extension to the aortic wall of a contiguous infective focus such as infected mediastinal lymph nodes or lung lesions. *Treponema pallidum* is a rare etiology today, with a historical importance. Aortic infection by unusual bacteria and nonbacterial (fungi) microorganisms is extremely rare; however, this possibility must be considered in immunocompromised patients (Gornik and Creager 2008). Infected (mycotic) aneurysms are uncommon, and they usually involve segments not commonly involved by atherosclerosis (Lee et al. 2008). Although the infraabdominal aorta is the most frequently involved segment of the aorta, there is also a combined involvement of the descending thoracic, thoracoabdominal, and suprarenal aorta (Oderich et al. 2001). Early changes of aortitis preceding aneurysm formation include an irregular arterial wall, periaortic edema as fat stranding or a hypoattenuating concentric rim at CT, a periaortic soft-tissue mass, and periaortic gas. Concentric or eccentric periaortic inflammatory soft tissue can develop, as a homogeneous contrast-enhancing mass at CT (Ting and Cheng 1997; Tsao et al. 2002; Azizi et al. 2004). The inflammatory mass can develop necrosis with a heterogeneous attenuation at CT, with rim enhancement or poor enhancement after administration of contrast material (Gomes and Choyke 1992). Periaortic mass and fat stranding are the most common imaging findings of infected aortic aneurysms, and they are found in 48 % of cases (Macedo et al. 2004). Periaortic gas is an uncommon feature (Vogelzang and Sohaey 1988; Macedo et al. 2004). At CT, an infected aortic aneurysm appears as a focal, contrast-enhancing dilatation, usually saccular. The lumen can be central or eccentric and it can be a single compartment or multiloculated. Disrupted arterial wall calcifications can occur adjacent to the infected aneurysm (Sueyoshi et al. 1998; Azizi et al. 2004). Calcification within the aneurysmal wall and thrombus within an infected aneurysm are uncommon (Gomes and Choyke 1992). An infected aneurysm can rapidly develop and enlarge (Sueyoshi et al. 1998; Macedo et al. 2004), and subsequently it can rupture due to high systemic arterial pressure.

Fig. 7 Axial (**a**) and sagittal MIP (**b**) CT images of a patient with Cogan syndrome, showing circumferential wall thickening of the normal caliber descending aorta (*arrow head* in **a**) and abrupt narrowing of the abdominal aorta distal to the mesenteric artery origin (*arrow* in **b**)

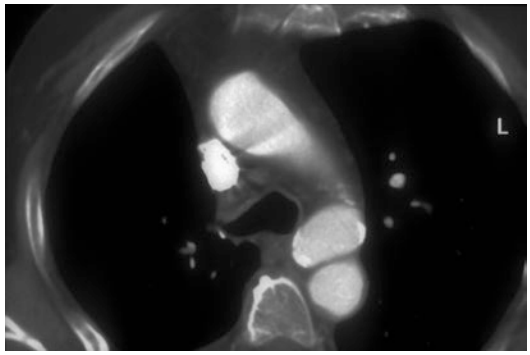

Fig. 9 Axial CT in a patient with chronic posttraumatic pseudoaneurysm of the aortic isthmus. There is no mediastinal hematoma and there are some calcifications along the aneurysmal wall

Fig. 10 Axial CT image at the aortic arch level in a patient with chronic dissection. The dilated aortic arch with intimal flap, false and true lumens are well demonstrated

Posttraumatic aneurysms or, *better*, *pseudoaneurysms*, following blunt trauma may result from rapid deceleration, which is the most accepted mechanism of injury (Agarwal et al. 2009), with shearing and bending stress on the aortic wall. According to this theory, during the sudden deceleration, the distal transverse arch moves forward while the proximal descending thoracic aorta remains stationary, held back by the ligamentum arteriosum and the intercostal vessels (Javadpour et al. 2002). Another proposed mechanism is the "osseous pinch," where an anteroposterior compression force results in posteroinferior displacement of the manubrium, first rib, and medial clavicle, which impinge on the aorta and compress it against the thoracic spine posteriorly (Crass et al. 1990). A third possible mechanism of aortic injury is represented by the sudden increase of intraluminal blood pressure due to trauma with the so-called water hammer effect (Creasy et al. 1997). The most common site of injury, seen in survived trauma victims, is the aortic isthmus (90 % of cases), followed by the ascending aorta and the descending aorta near the diaphragmatic hiatus (Mukherjee and Rajagopalan 2007). Chronic pseudoaneurysms develop in 2.5 % of patients who survive the initial trauma. These often calcify (Fig. 9), may contain thrombus (Heystraten et al. 1986), and have the potential to enlarge progressively, rupturing even years after the initial trauma (Posniak et al. 1990).

Aortic dissection is an abnormal passage of blood, through an intimal tear, into the media, producing a false lumen separated from the true lumen by an intimal flap. A previous aortic dissection, with a persistent false channel, may produce aneurysmal dilatation of the false lumen. These are false aneurysms, contained only by the outer media and adventitia, enlarging over time (Fig. 10).

1.5 Pitfalls

Normal aortic variants can mimic an aortic aneurysm. Three of these are ductus diverticulum, Kommerell's diverticulum, and aortic spindle.

1.5.1 Ductus Diverticulum

Ductus diverticulum consists of a convex focal bulge along the anterior undersurface of the isthmic region of the aortic arch (Gotway and Dawn 2003). Although ductus diverticulum is commonly believed to be a remnant of the closed ductus arteriosus, it has been suggested that this entity may actually represent a remnant of the right dorsal aortic root (Grollman 1989). It is particularly important to differentiate ductus diverticulum from a posttraumatic aortic pseudoaneurysm, which most commonly occurs at the aortic isthmus. In contrast to a pseudoaneurysm, ductus diverticulum has smooth margins with gently sloping symmetric shoulders and forms obtuse angles with the aortic wall (Gotway and Dawn 2003).

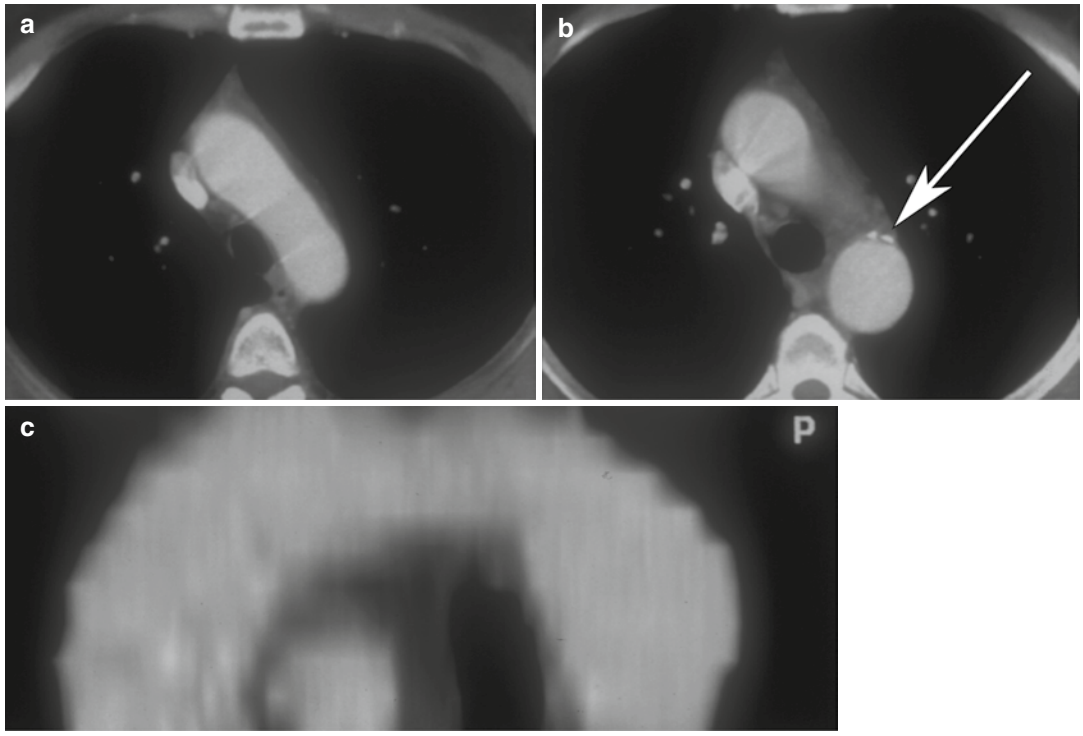

Fig. 11 Axial CT images (**a**, **b**) and sagittal–oblique MPR image (**c**) of aortic spindle, which is a normal mild dilation of the most proximal descending thoracic aorta. Note the calcific densities at the level of ductus arteriosus insertion (*arrow*)

1.5.2 Aortic Spindle

Aortic spindle is a smooth, circumferential bulge located below the isthmus, in the first portion of the descending aorta. It should not be confused with an aneurysm (Agarwal et al. 2009) (Fig. 11a–c).

1.5.3 Kommerell's Diverticulum

Right aortic arch (RAA) is an uncommon anatomical variant, occurring in about 0.1 % of the population (Shuford et al. 1986). Two main types are commonly seen: mirror-image branching (type I), commonly associated with congenital cyanotic heart disease, and aberrant left subclavian artery (LSA) (type II) (Yeo et al. 2015). Type II RAA is often accompanied by a Kommerell's diverticulum, an aneurismal diverticulum that develops at the origin of the LSA and the proximal aspect of descending aorta (Edwards 1948). Because of the atherosclerotic changes occurring in the arterial wall during life, in adults it is generally not possible to distinguish a true diverticulum (Kommerell's diverticulum, an embryonic remnant) from an acquired aneurysm of the origin of the aberrant LSA. Patients with type II RAA are often asymptomatic; they are diagnosed incidentally in adulthood or when complications arise from compression of the mediastinal structures, caused by a growing Kommerell's diverticulum (Hastreiter et al. 1966). However, it was originally described as a diverticular outpouching at the origin of an aberrant right subclavian artery with a left-sided aortic arch (Fig. 12a, b).

1.6 Complications

1.6.1 Rupture

The risk of rupture of TAAs increases with the size of the aneurysm (Gotway and Dawn 2003).

Indications for surgical treatment are summarized in the Guidelines of the American Heart Association (Hiratzka et al. 2010):

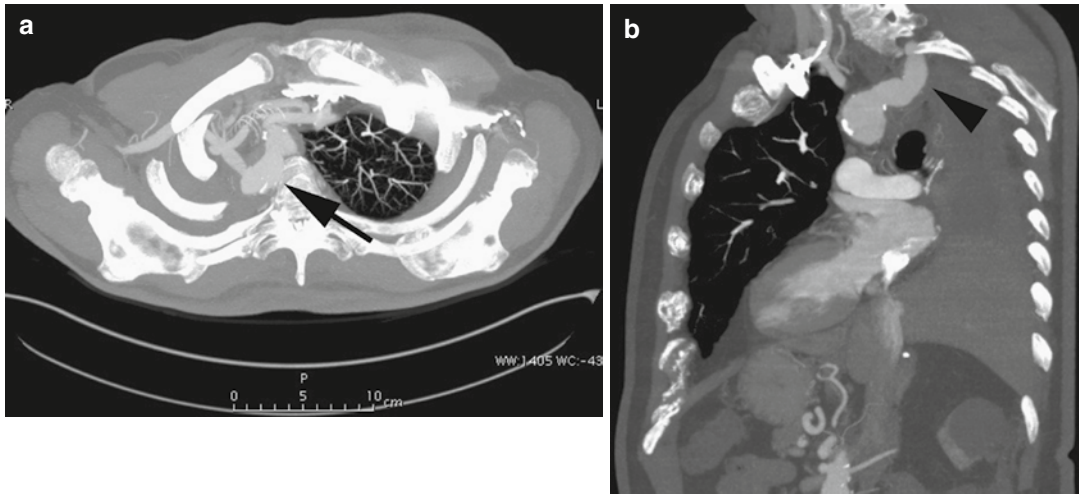

Fig. 12 Axial (**a**) and sagittal oblique (**b**) CT MIP images in a patient post-right pneumonectomy, with retroesophageal right aberrant subclavian artery with proximal aneurysmal dilation: Kommerell's diverticulum (*arrow* in **a**, *arrowhead* in **b**)

- Aortic size – ascending aortic diameter ≥5.5 cm or twice the diameter of the normal contiguous aorta; descending aortic diameter ≥6.5 cm; subtract 0.5 cm from the cutoff measurements if the following are present: Marfan syndrome, family history of aneurysm or connective tissue disorder, bicuspid aortic valve, aortic stenosis, dissection, and patient undergoing another cardiac operation; growth rate ≥1 cm/year
- Symptomatic aneurysm
- Traumatic aortic rupture
- Acute type B aortic dissection with associated rupture, leak, distal ischemia
- Pseudoaneurysm
- Large saccular aneurysm
- Mycotic aneurysm
- Aortic coarctation
- Bronchial compression by aneurysm
- Aortobronchial or aortoesophageal fistula

Contraindications are always individualized on patient's ability to undergo a major surgery. High-risk patients and elderly persons must be always considered for less invasive procedures. Patients with end-stage renal disease, respiratory insufficiency, cirrhosis, or other major comorbid conditions are the most critical.

CT is the modality of choice for identifying aneurysmal rupture. *CT findings of aneurysm rupture*. Thoracic aortic aneurysms can rupture into the mediastinum (Fig. 13a, b), pleural cavity, pericardium, or adjacent luminal structures such as the airways or the esophagus. CT findings are a high-attenuation hematoma on nonenhanced scans and an active contrast material extravasation from the aortic lumen on contrast-enhanced scans (Agarwal et al. 2009). An important imaging feature, in a contained rupture of TAA, is the "draped aorta sign": it occurs when the posterior wall of the aorta is not identifiable as distinct from adjacent structures or when it closely follows the contour of adjacent vertebral bodies (Halliday and al-Kutoubi 1996). *Imaging features suggestive of instability or impending rupture* include increased aneurysmal size, a low thrombus-to-lumen ratio, and hemorrhage into a mural thrombus (Rakita et al. 2007). Nonruptured aneurysms generally contain more thrombus than ruptured aneurysms and thrombus-to-lumen ratio decreases with the increase of the aneurysmal size (Pillari et al. 1988). It is intuitive that a thick circumferential thrombus is protective against rupture and an enlargement of the patent lumen is indicative of partial lysis of the thrombus, which predisposes an aneurysm to rupture (Pillari et al. 1988; Mower

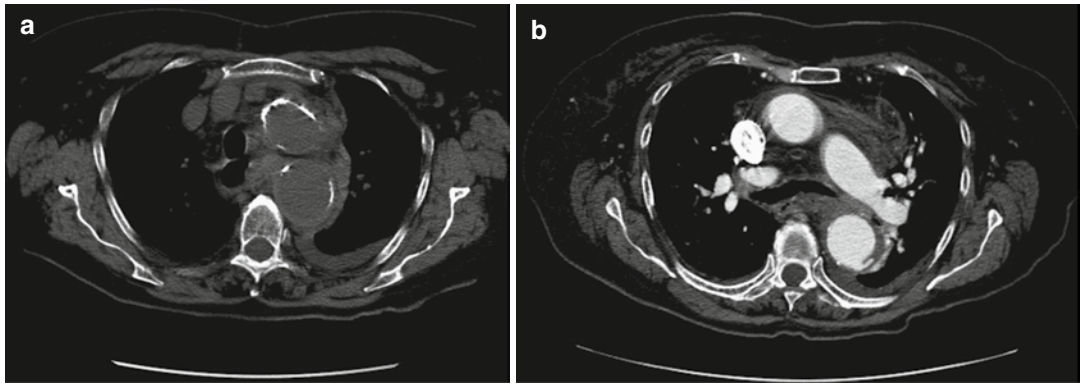

Fig. 13 Unenhanced (**a**) and enhanced (**b**) axial CT scan of a patient with ruptured aortic aneurysm. Unenhanced image (**a**) shows discontinuity in wall calcifications, high-attenuation hematoma, and draping of the posterior aortic wall. Enhanced image (**b**) shows active extravasation of contrast material into the thrombus. Both images demonstrate blood into mediastinum and left pleural cavity

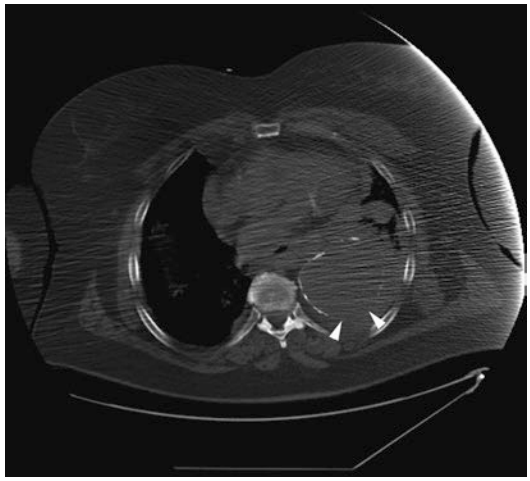

Fig. 14 Unenhanced axial CT sections of a patient with contained rupture of aneurysmal descending aorta. The discontinuity of wall calcifications is clearly shown on the posterior and lateral side of aorta (*arrow heads*)

et al. 1997). A focal discontinuity in the circumferential wall calcifications (Fig. 14) is more commonly observed in unstable or ruptured aneurysms (Siegel et al. 1994); this finding is really important when, in comparison with a previous CT, the area of discontinuity in mural calcifications is new. A well-defined peripheral crescent of increased attenuation (Fig. 15a, b) within the thrombus of a large TAA is a CT sign of acute or impending rupture (Mehard et al. 1994; Gonsalves 1999). This finding is best appreciated on unenhanced CT images. It represents an internal dissection of blood into the peripheral thrombus or into the aneurysm wall, when the ability of the thrombus to protect the aneurysm from rupture is shrinking (Arita et al. 1997). It is one of the earliest and most specific CT signs of the rupture process (Mehard et al. 1994; Siegel et al. 1994; Arita et al. 1997; Gonsalves 1999). A TAA can develop fistulous communication with the tracheobronchial tree and the esophagus. The aortobronchial fistula manifests clinically as hemoptysis (Lesko et al. 1997) and at CT as consolidation in the adjacent lung due to hemorrhage; the fistulous communication cannot be easily seen at CT (Coblentz and Sallee 1988). Most aortobronchial fistulas (90%) occur between the descending aorta and the left lung (MacIntosh et al. 1991). Aortoesophageal fistula is less common. It manifests clinically as hematemesis and dysphagia (Cho et al. 2004) and at CT as mediastinal hematoma, as an intimate relationship of the aneurysm to the esophagus, and, rarely, as contrast material extravasation into the esophagus (Green and Klein 2007).

1.6.2 Compression of Adjacent Structures

TAAs can produce symptoms by compressing adjacent structures, such as superior vena cava syndrome due to compression of the superior vena cava, stridor or dyspnea due to airway

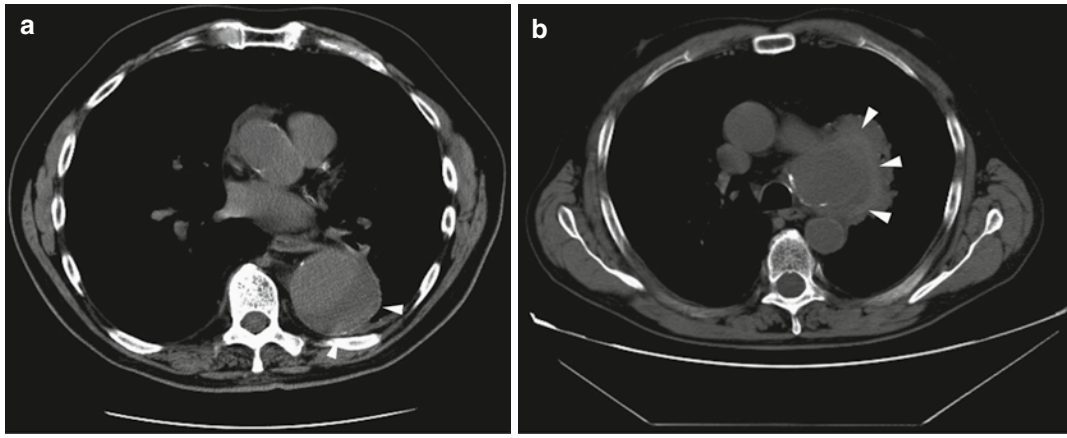

Fig. 15 Unenhanced axial CT scan of two different patients with hemorrhage into a mural thrombus. A peripheral crescent-shaped area of hyperattenuation (*arrow heads* in **a**, **b**), corresponding to the hematoma into the mural thrombus, is displayed in (**a**) a patient with impending rupture of an aneurysmal descending aorta with thrombus and (**b**) in a patient with contained rupture of aortic arch aneurysm into the mediastinum (**b**)

compression, hoarseness due to compression of the recurrent laryngeal nerve, and dysphagia due to esophageal compression (Posniak et al. 1990).

1.7 Clinical Presentation

Thoracic aortic aneurysms often grow slowly and usually without symptoms, making them difficult to detect. TAAs are usually found incidentally after chest radiographs or during other imaging studies. Most patients are hypertensive or can have a history of vascular disease in different districts, such as coronary or carotid arteries, but, in general, they remain relatively asymptomatic until the aneurysm expands.

The most common symptom is pain. Chest or back pain in presence of TAA is predictive of aortic rupture. Ascending aortic aneurysms tend to cause anterior chest pain, whereas arch aneurysms more likely cause pain radiating to the neck. Descending thoracic aneurysms more likely cause back pain localized between the scapulae. When located at the level of the diaphragmatic hiatus, the pain occurs in the mid-back and epigastric region; however, identifying the area of aortic involvement on the basis of the specific location of pain is not always reliable and can be misleading. Large ascending aortic aneurysms can cause superior vena cava obstruction with distended neck veins. Ascending aortic aneurysms also may develop aortic insufficiency and heart failure. Arch aneurysms, where stretching of the recurrent laryngeal nerves is present, may cause hoarseness. Descending thoracic aneurysms and thoracoabdominal aneurysms may compress the trachea and/or bronchi and cause dyspnea, stridor, wheezing, or cough. Compression of the esophagus results in dysphagia. They can also erode the surrounding structures and result in aortobronchial or aortoesophageal fistulas with, respectively, hemoptysis, hematemesis, or gastrointestinal bleeding. Erosion into the spine causes back pain or instability. Spinal cord compression or thrombosis of spinal arteries may result in paraparesis or paraplegia. Descending thoracic aneurysms may thrombose or embolize clot and atheromatous debris distally to visceral, renal, or lower extremity arteries.

The most common complications of TAAs are acute rupture and dissection with rupture into the pericardium, causing tamponade, or

dissection into the aortic valve, causing acute aortic insufficiency, or into the coronary arteries, causing myocardial infarction (Safi et al. 2012; Upchurch 2014).

1.8 CT Technique and CT Data Manipulation

In the clinical setting of acute nontraumatic chest pain, case history, physical examination, ECG, and laboratory risk markers should be immediately obtained. Chest X-ray is useful to rule out many nonvascular causes of acute chest pain such as pleural effusions, pneumothorax, etc. In the field of nontraumatic vascular emergencies, CT has a primary role with a sensitivity and a specificity near 100 % for acute aortic pathologies, while MRI is indicated mainly for follow-up of aortic pathologies due to longer scan time, limited availability, and increased cost (Nagpal et al. 2015).

The CT protocol starts with unenhanced scan to visualize intramural hematoma that can be misdiagnosed as atherosclerotic thrombus in the arterial phase CT scan (Chiu et al. 2013). The scan should be extended above the aortic arch (for aortic branches) and caudally to the femoral heads to cover aorta entirely. Then contrast-enhanced CT with high infusion rate (4–5 mL/s) is performed to achieve a target opacification of the aorta >250 HU, obtained in the arterial phase with a test bolus or a bolus-tracking technique. The contrast should be injected through the right upper extremity to avoid artifacts from left innominate vein in the area of the aortic arch. A saline flush of 30–40 mL should be injected following contrast medium to minimize streak artifact from superior vena cava (Weininger et al. 2011). Delayed images are recommended after stent–graft repair of aortic aneurysm to detect endoleaks (Task et al. 2014). ECG gating when available is very useful to avoid cardiac motion artifacts impairing the evaluation of thoracic aorta and coronary origin. ECG-gated imaging both in precontrast and in postcontrast CT, from above aortic arch to diaphragmatic hiatus, should be included in the standard protocols for thoracic vascular emergency. Prospective ECG gating is performed at mid-diastole if heart rate is <70 beats per minute, while it is acquired in end-systole in patients with heart rate >70 beats per minute (Abbas et al. 2014). High-quality images of aortic root and proximal coronary tracts can be obtained without ECG gating using newer CT scanners (128 slice CT) with fast gantry rotation time and iterative reconstruction algorithm to reduce both X-ray dose and contrast media volume (Russo et al. 2015).

MDCT images are initially evaluated in axial sections, but two-dimensional and three-dimensional reformatting techniques such as multiplanar reformation (MPR), maximum intensity projection (MIP), and virtual rendering (VR) allow better diagnosis of aortic pathology. In particular to obtain correct measurement of the aortic diameters, it is necessary to use MPR images perpendicular to the centerline of the aortic lumen to avoid overestimation (Fig. 16a). Measurements of the aortic lumen on the transaxial CT images are incorrect when the central axis of the aorta is not perpendicular but oblique to the transaxial CT image (Fig. 16b).

MIP is a useful tool to display vascular map (Fig. 17) but doesn't demonstrate the 3D relationship with nonvascular structures, while volume rendering (VR) allows to display vascular anatomy and provides, at the same time, definition of the surrounding structures (Fishman et al. 2006) (Fig. 18). It is the only way to transfer to the referring clinician the 3D perspective of the aortic aneurysm.

A standard report describing thoracic aorta should include the following measurements (Agarwal et al. 2009):

- Sinus
- Sinoaortic junction
- Midascending aorta
- Proximal aortic arch
- Midaortic arch
- Proximal descending aorta
- Aorta at diaphragm

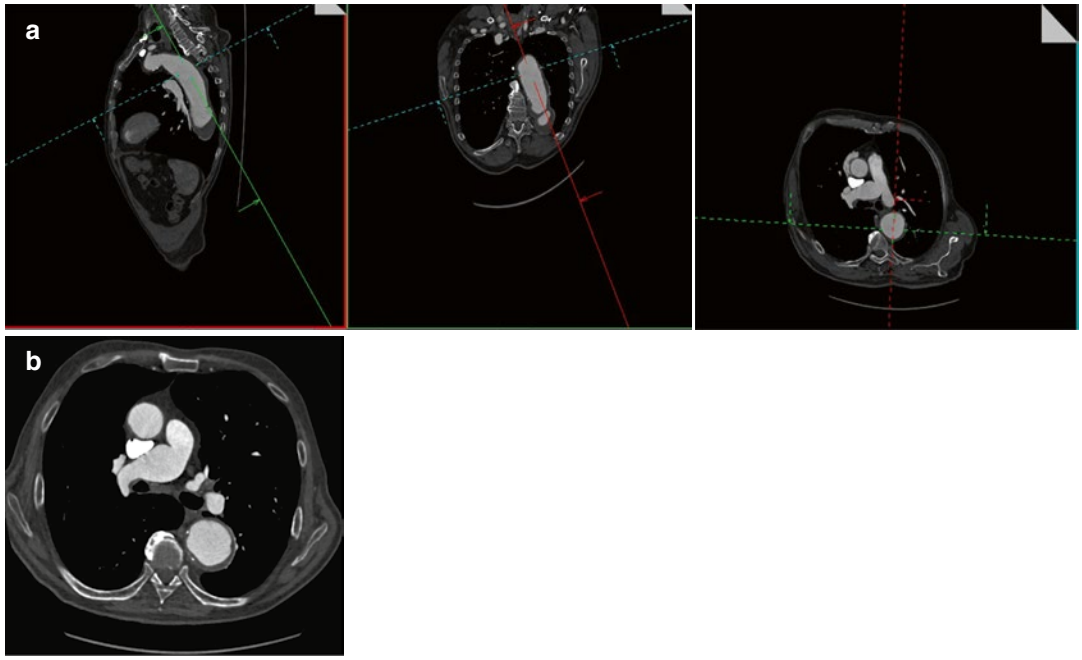

Fig. 16 A 77-year-old woman with descending aortic aneurysm. Multiplanar postcontrast CT images show the correct (**a**) technique of wall-to-wall measurement of the descending aortic aneurysm perpendicular to its center line. Pure axial postcontrast CT image of the same patient shows the incorrect (**b**) measurement technique of the aneurysm due to overestimation

Every report of an aneurysmal thoracic aorta must include the relationships between the aneurysm and the aortic branches, to assess the possibility of endovascular repair. Minimum length of 15 mm from aortic lesion and left subclavian artery/celiac trunk and maximum aortic landing zone diameter of 40 mm without circumferential thrombus within the landing zone are essential to perform endovascular procedure (Garzón et al. 2005).

2 Thoracic Aortic Thrombosis

2.1 Introduction

With the advent of recently developed imaging techniques and the routine exploration using TEE after any embolic events, the presence of thrombi in the aorta has been increasingly identified. The primary source of peripheral arterial embolism (PAE) is cardiac in more than 85 % of cases (Reber et al. 1999). Among noncardiac sources, the aorta has been reported in up to 5 % of cases to be the origin of PAE (Gagliardi et al. 1988).

Thrombus formation can be found both in atheromatous and in apparently normal aorta.

2.2 Definition, Etiology, and Clinical Presentation

Aortic mural thrombi usually arise as a consequence of preexisting aortic pathology. Thrombogenic lesions such as aneurysm, complex atherosclerotic plaque with protruding atheromas, and/or dissection are found to underlie the vast majority of aortic thrombi (Rossi et al. 2002).

Fig. 17 MPR sagittal view with MIP CT image of thoracic aorta aneurysm

Common well-recognized embolic sources of aortic thrombosis include intracardiac thrombus or myxoma.

Thrombi in the thoracic aorta are even much less common, particularly in apparently normal aorta. It has been initially associated to premature atherosclerosis, as a result of prior trauma, but some authors suggested as a separate clinical entity.

Primary aortic mural thrombus (PAMT) is defined as a thrombus formation in a morphologically normal aorta without any evidence of cardiac source.

In 1958, H. Gaylis described the first case of PAMT: the thrombus was located in the abdominal aorta (Gaylis 1958). Later, Machleder et al. confirmed this clinical entity: in 10,671 consecutive autopsies, he found 95 cases of mural thrombus of the thoracoabdominal aorta and reported an incidence of 0.45 % (48 cases) of nonaneurysmal aortic mural thrombus, with 17 % of these patients having evidence of distal embolization (Machleder et al. 1986).

Because the disease is mostly asymptomatic, the true incidence of PAMT remains unknown. In two large series that evaluated patient with PAE, the incidence reported was higher and varies from 5 to 20 % (Verma et al. 2014).

Verma et al. identified 19 PAMT in a retrospective study of 88 patients who underwent extensive evaluation of acute occlusion of extremities or visceral arteries. Mural thrombus was located in the thoracic aorta in ten patients (52 %) and in the abdominal aorta in nine (48 %) (Verma et al. 2014).

The most frequent thoracic location of PAMT is the region of the aortic isthmus and the portion distal to the aortic arch, at the side opposite to the origin of the subclavian artery (Choukroun et al. 2002). Also, localization of aortic thrombus in the ascending aorta has been described (Pousios et al. 2009).

PAMT is more frequent in young women, and it has been associated in patients with essential thrombocytosis (Fang et al. 2001) and Crohn's disease (Lehmann et al. 2001). Smoking, steroid therapy, elevated fibrinogen levels and/or hypercoagulability, and numerous underlying pathologies have been reported.

Underlying pathologies described in morphologically normal thoracic aortic thrombosis
Predisposing factor[a]
Essential thrombocythemia
Protein C or S deficiency
Antiphospholipid syndrome
Heparin-induced thrombocytopenia
Hyperhomocysteinemia
Iatrogenic (e.g., intra-aortic balloon pumping)
Aortic wall tumor
Cancer
Chemotherapy
Homozygous plasminogen activator inhibitor type 1 (PAI-1)
Factor V Leiden
Familiar dysfibrinogenemia
Antithrombin III deficiency
Blunt aortic trauma
Drug abuse
Elevated factor VIII
Aspergilloma
Rheumatic disease
Crohn's disease (Lehmann et al. 2001)
Pancreatitis (Verbeeck et al. 2014)

[a]Modified from Tsilimparis et al. (2011)

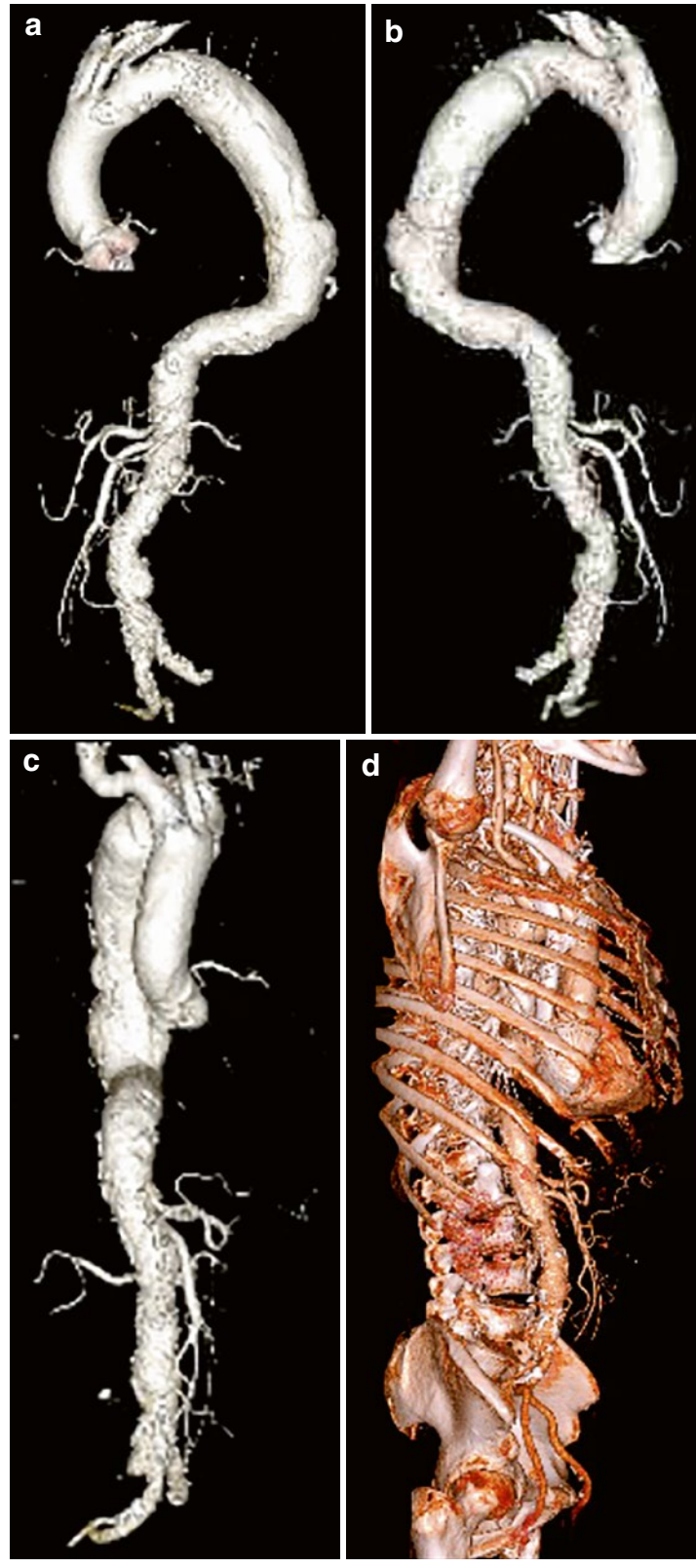

Fig. 18 3D volume-rendered CT images of thoracic aorta aneurysm in lateral (**a**, **b**) and frontal view (**c**). In (**d**) 3D volume-rendered CT image of the same patient without bone elimination

In all patients who underwent surgery, histopathological examination revealed microscopic features of atherosclerosis limited to the insertion site (Laperche et al. 1997).

Clinical presentation is variable and mainly characterized by peripheral or mesenteric embolization arising from detachment of large thrombi within the visceral aortic segment. In some cases, cerebral transient ischemic attack, acute pancreatitis, and exacerbation of Crohn's disease symptoms are associated.

2.3 Diagnostic Workup

The diagnostic workup for aortic thrombosis includes TEE and cardiologic evaluation combined with imaging modalities (CT and/or MRI) and laboratory screening test for hypercoagulable disorders.

The differential diagnosis of PAMT must be established with primary aortic tumors (Thalheimer et al. 2004) and certainly with aortic dissection because of the urgent therapeutic implications.

A diagnosis can be achieved by TEE, CT, MRI, and digital subtraction angiography (DSA). Currently, because of the rarity of the disease, there are no robust studies comparing the various imaging techniques; consequently, there is a lack of consensus on the relative role (comparative effectiveness) of these imaging modalities and on the ideal way of managing PAMT.

Review of published data on aortic mural thrombus until 2014 revealed fewer than 250 cases, the majority of which were single case reports (Fayad et al. 2013).

Several authors have earlier reported TEE to be an adequate method for detecting PAMT (Lau et al. 1997) with some suggesting TEE to be comparatively more sensitive than CT or MRI (Tunick et al. 1991).

However, these studies were published before recent advancements in CT and MRI imaging with high- spatial resolution images. Currently, the recommended approach for a complete diagnostic workup requires the synergistic use of at least two modalities, TEE (mainly for exploration of cardiac cavities) and CT or MRI for the detection of thrombi and the evaluation of thrombus and of the entire aorta (Tsilimparis et al. 2011; Verma et al. 2014; Abissegue et al. 2015).

TEE allows a thorough examination of both the heart and the thoracic aorta. It plays a key role because it is the gold standard (sensitivity > 95 %) in identifying a cardiac source (thrombi in atrial fibrillation, valvulopathy, myocardial infarction) of embolism (85 % of all arterial thrombosis). Cardiac CT and of course cardiac MR have been proposed as an alternative method (Romero et al. 2013; Shapiro et al. 2007; Goldstein et al. 2015). On the other hand, echocardiography is less consistently able to image the distal ascending aorta, aortic arch, and descending thoracic aorta. To image these segments, CT and MR are preferred (Goldstein et al. 2015).

CT is the imaging modality of choice for diagnosis of most aortic pathologies, preoperative planning, and follow-up after invasive or medical treatment. This status reflects its widespread availability, accuracy, and applicability.

PAMT is recognized on CT as a hypodense endoluminal filling defect in a non-aneurysmatic and non-atherosclerotic aorta (Fig. 19a).

Multiplanar reconstructions obtained are very effective at distinguishing a subtle and pedunculated thrombus from intimal flaps, tears, or dissection (Fig. 19a–e).

The morphologic feature of the thrombus (sessile vs. pedunculated), the location, and the length of the aortic segment involved (Fig. 20a–c) could be predictors of embolic potential of such a lesion (Verma et al. 2014; Karalis et al. 1991).

Furthermore, CT allows simultaneous imaging of vascular structures, including the vessel wall and of viscera, and can assess severe complications due to distal vessel embolism detecting visceral malperfusion, splenic, hepatic, renal, or intestinal infarction or peripheral arterial occlusion (Vernhet et al. 2004).

Noteworthy, CT is able to demonstrate both aortic source of embolism (atherosclerotic plaque or rare aortic tumors) and extra-aortic diseases associated with PAMT (Crohn's disease, pancreatitis, or malignancies) (Verbeeck et al. 2014).

MRI is a second-line imaging modality in assessing aortic disease because of some

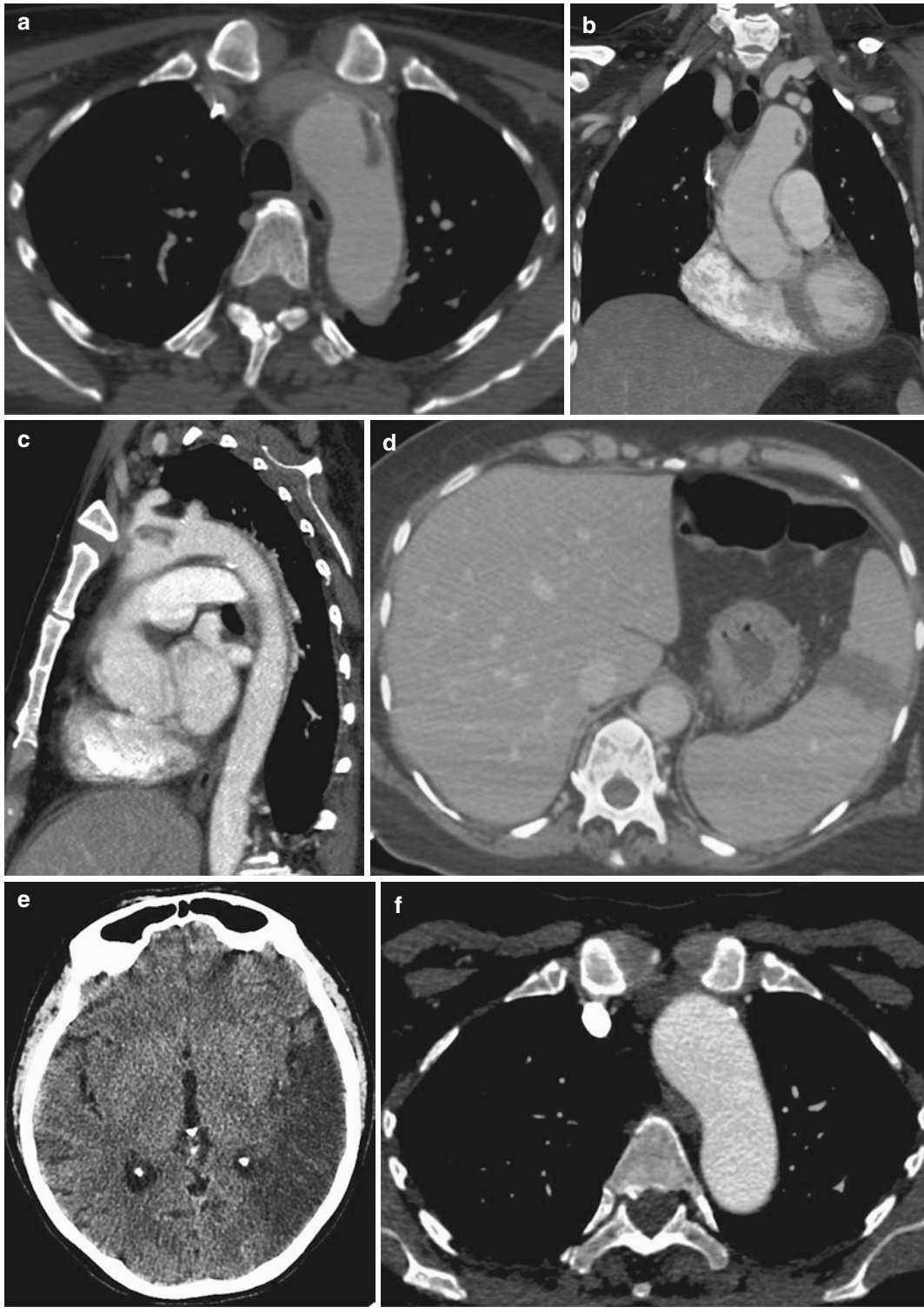

Fig. 19 A 50-year-old woman presented to ED with abdominal pain. After a negative abdominal US, she developed aphasia and underwent head CT and TEE investigation. On the basis of TEE, thoracic aortic dissection was suspected. CT demonstrates a filling defect in a non-aneurysmatic aortic arch adjacent to a small calcified plaque (**a**) and a splenic infarction (**d**). Reformatted images (**b**, **c**) help in differentiating floating thrombus from intimal flap. Head CT demonstrated a left temporal lobe ischemia (**e**). After anticoagulant therapy, the thrombus disappeared (**f**)

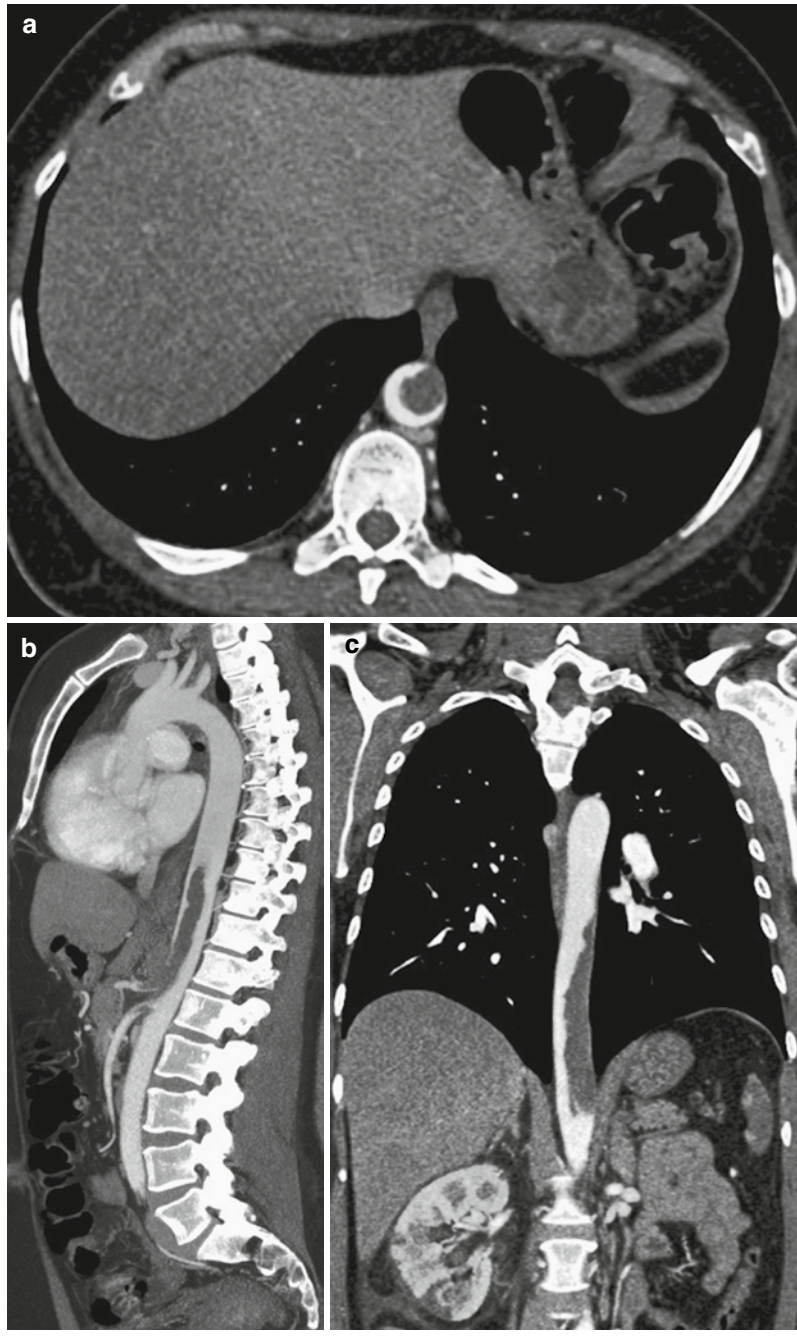

Fig. 20 Axial CT image (**a**) demonstrates an endoluminal filling defect in the non-aneurysmatic descending aorta of a young woman. Sagittal (**b**) and coronal (**c**) reformatted images demonstrate the features of the sessile thrombus located in the descending thoracic aorta and extended to celiac and superior mesenteric arteries and causing right kidney infarctions

disadvantages: the examination time is longer than CT; it benefits from patient cooperation (breath hold), in the turbulent flow that accompanies many cardiovascular diseases may suffer from artifacts that generate false-positive images and is limited in emergency situations. On the other hand, MRI is excellent for differentiating primary intramural hematoma from atherosclerotic plaque and intraluminal thrombus. MRI can noninvasively distinguish various components of the plaque, such as fibrous cap, lipid core, and thrombus, thereby assessing plaque stability (Oppenheim et al. 2009). Furthermore, MRI offers the possibility of diagnosing primary aortic or cardiac neoplasm in the differential diagnosis with thrombi.

Myxomas are the most common type of primary cardiac tumor (25–50 %), and in 75 % of cases, they originate from the left atrium. In MRI, these benign lesions are hypointense or isointense in T1-weighted sequences and hyperintense in T2-weighted sequences, with inhomogeneous contrast enhancement pattern. This is useful in the differential diagnosis with thrombi that should not enhance (Motwani et al. 2013).

Aortic sarcoma and cardiac angiosarcoma are very rare and aggressive malignant neoplasms that often are already metastatic at the diagnosis. Aortic sarcomas are broadly categorized as either primarily luminal or primarily mural. The luminal type often forms intraluminal polyps or extends along the intima causing peripheral emboli or aortic obstruction. The mural type originates from the media or adventitia and usually extends beyond the aorta (Bendel et al. 2011).

MRI shows inhomogeneous signal intensity in T1-weighted and T2-weighted sequences (sometimes can appear hyperintense in T1-weighted sequences with fat suppression due to its methemoglobin content in case of subacute hemorrhage), with inhomogeneous enhancement in postcontrast images.

Von Falck et al. observed in three patients with sarcomas of the aorta a pedunculated appearance ($n = 2/3$), an atypical location for a thrombus ($n = 2$), an expansion beyond the vessel wall ($n = 1/3$), contrast enhancement in MRI ($n = 2/2$, MRI was available in two patients) or MDCT ($n = 1/1$, MDCT was available in one patient), and metabolic activity as demonstrated by F-18 FDG PET/CT ($n = 1/1$; SUVmax = 3.6–5.5, PET was available in one patient) (von Falck et al. 2013).

2.4 Treatment

How to treat this potentially devastating aortic thrombus is a management dilemma.

Embolism from large vessel thrombi is potentially lethal, and it has been managed surgically in a few reported cases (Lehmann et al. 2001; Rossi et al. 2002; Mohammadi et al. 2007). Also, thrombolysis, thromboaspiration, and endovascular stent grafting have been utilized (Hausmann et al. 1992; Fueglistaler et al. 2005). Therefore, no guidelines for its management have been established.

In recent years, medical management of large intra-aortic thrombosis with systemic long-term anticoagulation with warfarin has been proposed with good results. Failure to continue warfarin therapy resulted in problems. Surgical treatment should be reserved only for selected cases of recurrent embolism or persistent symptomatology related to thrombus despite proper anticoagulation.

3 Aortobronchial Fistula

3.1 Definition, Etiology, and Clinical Presentation

Aortobronchial fistula (ABF) is a direct communication which occurs between the aorta and the bronchial tree. ABF was first described by Keefer in 1934 (Demeter and Cordasco 1980; Keefer 1934).

Primary ABF occurred rarely in patients who have no history of surgical intervention although the true incidence could be underestimated because more than 30 % are diagnosed at autopsy (Léobon et al. 2002). ABF is almost always associated to an underlying TAA. Compression of the tracheobronchial tree by enlargement of the TAA or low-grade inflammatory process associated may induce pressure necrosis, which can lead to erosion of both the aortic and bronchial walls.

The left bronchial tree is more frequently involved in ABF with the communication usually localized between the aneurysm and the membranous wall of the bronchus.

Secondary ABF is relatively more frequent and occurs postoperatively, after the implantation of a prosthetic vascular graft in the thoracic aorta (Favre et al. 1994; MacIntosh et al. 1991; Dorweiler 2001).

ABF can also occur in case of pseudoaneurysm as complication of aortic coarctation repair by means of patch aortoplasty (Milano et al. 1999) or after deployment of self-expanding bronchial stent to relieve extrinsic compression of a left main bronchus by a dissected descending aorta (Katayama et al. 2000).

When fistula between the aorta and bronchial lumina is created, patient presents hemoptysis that is usually massive, but occasionally is minor and intermittent. Hemoptysis is defined as the expectoration of blood that originates from the tracheobronchial tree or pulmonary parenchyma. Although hemoptysis is not specific to ABF, it is the most common presenting symptom and occurs in over 95 % of cases (Demeter and Cordasco 1980). Common causes of hemoptysis include chronic bronchitis, bronchiectasis, pneumonia, fungal infections, tuberculosis, malignancy, and rarely pulmonary vasculitis (Ketai et al. 2014). The differential diagnosis is broad; the severity and the prognosis of the underlying disease are very variable. Most cases are benign and hemoptysis is a self-limiting event.

ABF must be strongly suspected when hemoptysis occurs in a patient who has had a TAA or has undergone to thoracic aortic surgery. Even the first of hemoptysis can be fatal, and a very high mortality rate accompanies recurrence, which can be a consequence of lysis or displacement of the temporary clot.

3.2 Diagnostic Workup

Diagnostic modalities for studying hemoptysis include chest radiography (CXR), bronchoscopy, CT, and DSA (Larici et al. 2014).

Life-threatening hemoptysis is rare and requires urgent investigations and appropriate treatment. The diagnosis of the vascular source of hemoptysis should be clarified in order to decide the treatment (surgical or endovascular).

In 95 % of cases of hemoptysis, systemic arterial supply to the lungs (mainly bronchial arteries) is the origin of the bleeding (Bruzzi et al. 2006). Exceptionally, hemoptysis is related to the aorta. Unfortunately, the ability to diagnose ABF is further confounded by the lack of a diagnostic test that can definitely demonstrate the fistula (Riesenman et al. 2009). Chest radiograph (CXR) is the initial imaging modality. The sensitivity of CXR in this clinical context is not high. Radiography can help to lateralize the bleeding and can often help to detect underlying parenchymal and pleural abnormalities (Hsiao et al. 2001). Lung consolidation, resulting from hemorrhage into lung, is the most common radiographic finding in aortobronchopulmonary fistula (Coblentz and Sallee 1988). A more specific finding is the demonstration of a thoracic aortic aneurysm, which can be seen on the chest radiograph in 46 % of cases.

If CXR demonstrates an aortic dilatation combined with an opacification of the airspace that obscures the adjacent outline of the arch or the descending aorta, a diagnosis of ABF should be suspected even in case of no previous history of aortic surgery.

With minor and intermittent hemoptysis, the diagnosis may go unrecognized. This may end in death as in some reports when the minor and intermittent hemoptysis lead to the mistaken diagnosis of bronchitis (Demeter and Cordasco 1980; Oldham et al. 1983; Garrett et al. 1965; Graeber et al. 1980). CT evaluation is mandatory.

CT can identify the site of bleeding as accurately as bronchoscopy and detect underlying disease with high sensitivity (Revel et al. 2002). The site of hemorrhage is usually localized on the basis of the presence of liquified material in segmental and lobar bronchi and of hazy consolidation or ground-glass infiltrates in the lung parenchyma, findings that represent intra-alveolar hemorrhage (Bruzzi et al. 2006).

When these findings are mainly adjacent to the aorta, radiological features of TAA must be accurately evaluated (Fig. 21a, b, d). Although CT will rarely show the communication between the lung and the aorta because the fistula is

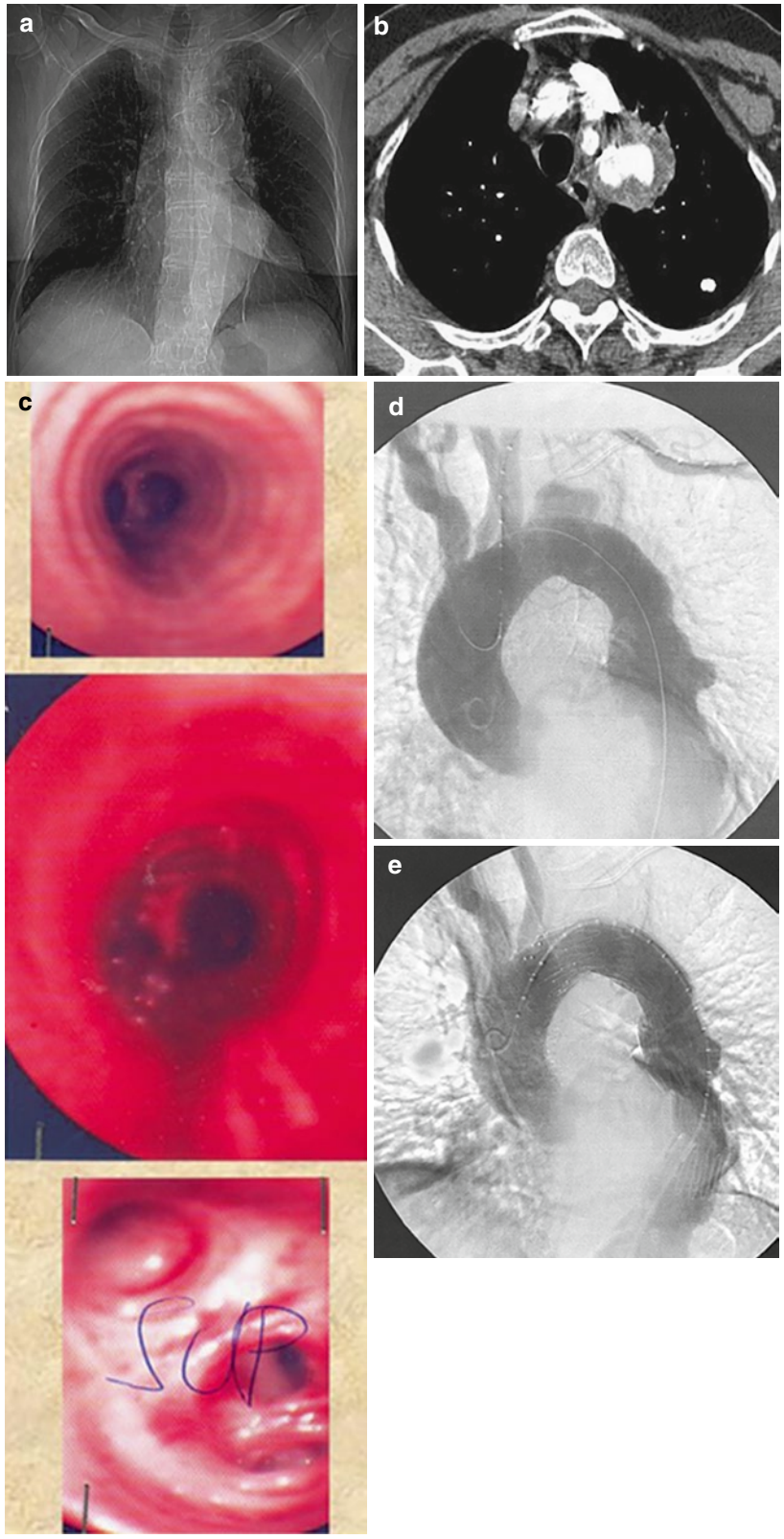
a
b
c
d
e

usually filled with clot (Graeber et al. 1980), the diagnosis of ABF is highly suggestive in this clinical setting (Pinilla et al. 2006).

Bronchoscopy (Fig. 21c) and DSA are often part of the evaluation of hemoptysis, and bronchoscopy could be directly visualize the fistula; however, both of these modalities often can fail to demonstrate the ABF (Liu et al. 2004) and may potentially induce massive hemorrhage dislodging clots overlying the fistula tract (Picichè et al. 2003).

4 Aortoesophageal Fistula

4.1 Definition, Etiology, and Clinical Presentation

Aortoesophageal fistula (AEF) is an uncommon cause of massive gastrointestinal hemorrhage that is associated with high morbidity and mortality and consists in direct communication between aorta and esophagus.

AEFs are classified as either primary or secondary. The main causes of primary AEFs are the erosion of a thoracic aortic aneurysm, foreign body ingestion such as bone from animal foods or sharp metal objects, and advanced esophageal malignancy (Lee et al. 2010; Hollander and Quick 1991; da Silva et al. 1999; Nandi and Ong 1978).

Cases of esophageal diverticulum associated with a secondary infective TAA complicated by AEF development have also been reported (Yasuda et al. 2002).

Secondary AEF occurs as complications of aortic reconstructive surgery with or without the placement of an aortic stent graft.

The exact pathophysiological mechanism of AEF remains unknown. Investigators suggested that the pathogenesis is related to esophageal ischemia secondary to elevated pressure in the posterior mediastinum, inflammation of the resorbed hematoma, mechanical compression by a large aneurysm and secondary erosion, or the geometric change in the aortic arch and the descending aorta after TEVAR. The radial force of the graft against the native aortic wall can be a causative factor (Okita et al. 2014; Hollander and Quick 1991; Czerny et al. 2014; von Segesser 1997). Primary infection or inflammation of the aneurysmal wall is also a potential cause of AEF (Hollander and Quick 1991).

The number of primary AEF resulting from aneurysm rupture is in apparent decline for the emerging use of open surgical and endovascular treatment of TAA at early stages. However, with the growing number of surgical repair of thoracic aneurysms and interventional procedures, postoperative AEF has become increasingly evident over time. The incidence of AEF as complication of open repair of the thoracic and thoracoabdominal aorta ranges from 0.5 to 1.7 % (Kieffer et al. 2003; Lawrie et al. 1994; Svensson et al. 1993). Diagnosis of AEF is rarely characterized by massive hematemesis. Patients usually present with the classic manifestations of midthoracic pain, sentinel arterial hemorrhage, and exsanguination after a symptom-free interval (Chiari's triad). In a few cases, AEF can be suspected on the basis of isolated sepsis or septic embolism in a lower extremity (Seymour 1978).

Other suggestive findings include dysphagia and/or chest pain and previous surgery involving the thoracic aorta (Kieffer et al. 2003).

4.2 Diagnostic Workup

Most diagnostic tests have significant individual limitations. The identification of massive upper

Fig. 21 A 70-year-old woman with intermittent hemoptysis. Chest radiography (scout view) demonstrated ill-defined aortic arch outline with calcified plaque (**a**). CT axial image detected multiple ulcerated atheromatous plaque (**b**) and an aneurysmatic aortic arch. Bronchoscopy (**c**) found a blood clot in the upper left lobe bronchus close to the aortic arch. TEVAR treatment was indicated: DSA demonstrated multiple aortic parietal bulging (**d**), the bigger in the aortic arch before the placement of the graft (**e**). After TEVAR, hemoptysis stopped

gastrointestinal hemorrhage that is bright red and arterial in nature is characteristic. Endoscopy of the upper gastrointestinal tract might aid in the detection of fistula. Endoscopic findings may be directly due to visualization of pulsatile blood into the esophagus or a pulsatile adherent blood clot. More subtle findings during endoscopy might point in direction of a fistula, such as submucosal hematoma shown as a blue-gray discoloration of the esophageal wall. However, the sensitivity of detection of fistulae via endoscopy is a mere 38 % (Perdue et al. 1980).

Although no single imaging modality demonstrates AEF with sufficient sensitivity and specificity, computed tomography (CT) is the imaging modality of choice for evaluations in the emergency setting (Figs. 22a–c and 23a–c). The clinical manifestations are often crucial to the diagnosis of aortoenteric fistula (Vu et al. 2009).

The most specific but quite rare sign of AEF is the identification on CT of direct extravasation of contrast from the aorta into the esophagus (Fig. 22d, e) (Vu et al. 2009; Raman et al. 2013), but during the symptom-free interval, radiological evidence of AEF may be absent due to the transient clot formation (Khawaja and Varindani 1987).

Similarly, the leakage of enteric contrast directly into the periaortic space is a highly specific sign, but extremely rare (Fig. 22f).

Other important signs to assess are esophageal wall thickening, effacement of the periaortic fat plane, and periaortic soft tissue/fluid.

Identification of an aortic aneurysm or a penetrating atherosclerotic ulcer adjacent to a mediastinal soft-tissue mass or to a mediastinal hematoma is helpful for ascertaining the precise location of a primary aortoenteric fistula (Hughes et al. 2007).

The diagnosis of secondary AEF is dependent on a number of other nonspecific, but suggestive, findings, including effacement of the periaortic fat plane (Fig. 22b), focal thickening and tethering of the esophageal wall immediately adjacent to the aorta (Fig. 22d, e), periaortic free fluid and soft-tissue thickening, and disruption of a graft (Fig. 22d, e) or significant graft migration (Low et al. 1990).

However, CT normal findings in the immediate postoperative period should not be misinterpreted as a fistula. Perigraft soft-tissue edema, fluid, and ectopic gas may be normal immediately after surgery. After 3–4 weeks, any ectopic gas is abnormal and should be considered a sign of perigraft infection and possibly fistulization (Hughes et al. 2007; Vu et al. 2009). The perigraft soft-tissue thickening, fluid, or hematoma should resolve within 2–3 months after surgery (Vu et al. 2009).

Because of their overlapping CT features, aortoenteric fistula and perigraft infection may be difficult or impossible to differentiate. However, the specific CT findings that correlate strongly with the presence of aortoenteric fistula include ectopic gas (Fig. 22b), focal esophageal wall thickening, breach of the aortic wall, and extravasation of contrast material into the esophageal lumen (Fig. 22d, e) (Low et al. 1990; Hughes et al. 2007; Hagspiel et al. 2007; Vu et al. 2009).

Esophageal ingested foreign body such as bones is easily detectable (sensitivity 100 %) by CT (Fig. 22c) even if they migrated in the mediastinum and both radiography and endoscopy are negative (Marco De Lucas et al. 2004).

Foreign bodies in the thoracic esophagus tend to be lodged at the level of the left primary bronchus, where the aortic arch presses against

Fig. 22 Primary AEF fistula in a 65-year-old woman with hematemesis and a history of ingested bone. A pseudoaneurysm of the descending thoracic aorta is visible in the arterial phase (axial image **a**). Ectopic gas is detectable in the mediastinal hematoma that surrounds the pseudoaneurysm (**b**, venous phase) and occupies the fat plane between the esophagus and the aorta. Parasagittal MPR (**c**) demonstrates both the small foreign body (*arrow*) close to the left main bronchus and the pseudoaneurysm. Patient developed also a severe mediastinitis and three months post-TEVAR she had hematemesis. Axial (**d**) and coronal reformatted (**e**) images demonstrate contrast leakage in the esophagus and AOF localized where the esophageal wall is tethered to the aorta. Although the infected graft was removed and with the placement of esophageal stent, the fistula was fatal. Radiograph (**f**) demonstrates oral contrast leakage in the mediastinum

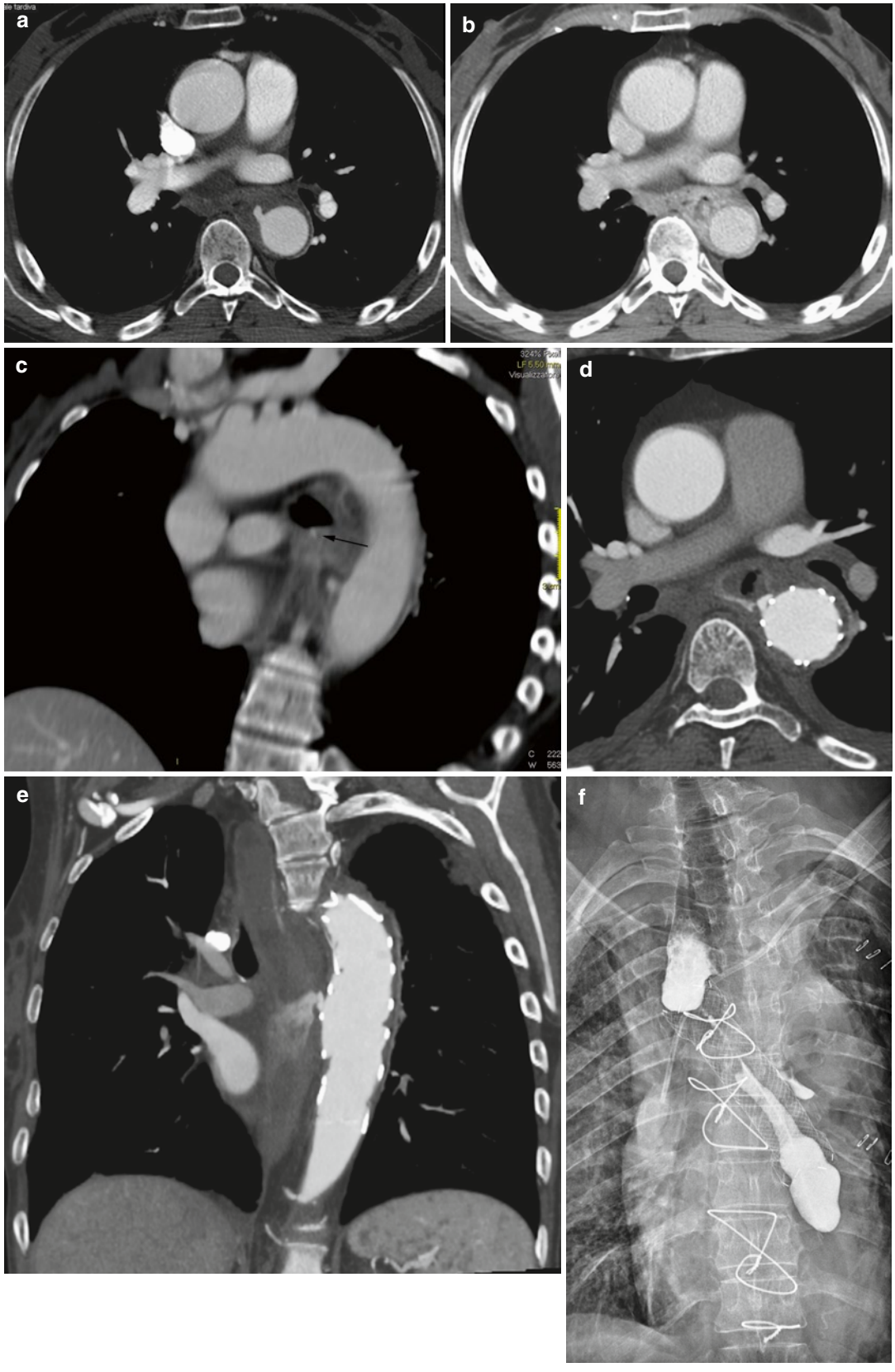
a
b
c
d
e
f

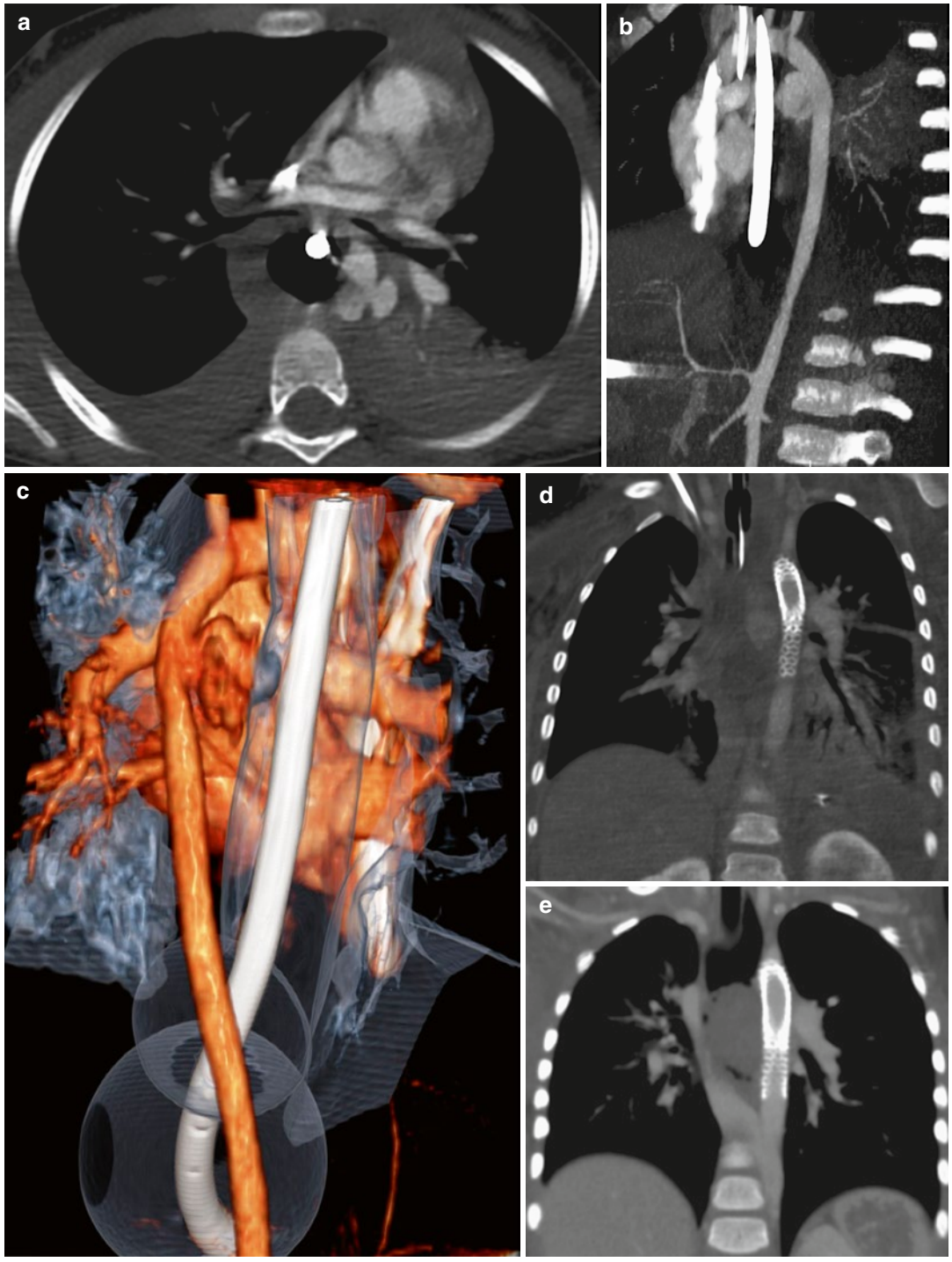

Fig. 23 Primary AEF in a 4-year-old patient presenting with massive hematemesis. Axial CT image (**a**), sagittal MIP (**b**), and VR posterior view (**c**) demonstrate a large pseudoaneurysm. Esophagus is distended by an insufflated Sengstaken–Blakemore balloon (**c**). Immediately after TEVAR, CT coronal image (**d**) demonstrated the excluded pseudoaneurysm, filled with residual contrast, which in the following CT evolved in a large hypodense hematoma (**e**) with narrowing the adjacent esophageal lumen (**f**)

Fig. 23 (continued)

the esophagus and creates a relatively narrow lumen (Wei et al. 2015).

Interestingly, Wei Y. et al. analyzed the clinical data of 22 patients with ingested foreign bodies retrospectively and developed a classification system based on CT findings for esophageal injuries and used this system and the clinical presentation to guide treatment. Depending on the CT findings, the esophageal injuries were divided into four grades: Grade I, non-penetrating injury; Grade II, penetrating injury with minimal infection; Grade III, potential AEF; and Grade IV, definite AEF (Wei et al. 2015). CT findings in Grade III were suggestive of esophageal perforation and severe intrathoracic infections such as mediastinitis, chest empyema, and abscess with foreign body close to the aorta (<2 mm). In Grade IV, CT findings were aortic wall perforation, pseudoaneurysm, and mediastinal abscess.

4.3 AEF and ABF Treatment

Surgical treatment of AEF and ABF requires replacement of the thoracic aorta associated with adjunctive procedures to repair the esophageal or tracheobronchial lesion with a high rate of perioperative mortality and morbidity. Recently, the use of TEVAR (Figs. 21e and 23d, e) has been proposed as mini-invasive treatment. Although the excellent technical result in the immediate postoperative period, there are several limitations due to the high risk of contamination of the graft. For this reason, TEVAR should be considered as a "bridge" intervention to the open treatment.

References

Abbas A, Brown IW, Peebles CR et al (2014) The role of multidetector-row CT in the diagnosis, classification and management of acute aortic syndrome. Br J Radiol 87:20140354. doi:10.1259/bjr.20140354

Abissegue YG, Lyazidi Y, Chtata H et al (2015) Acute systemic embolism due to an idiopathic floating thrombus of the thoracic aorta: success of medical management: a case report. BMC Res Notes 8:181

Agarwal PP, Chughtai A, Matzinger FRK, Kazerooni EA (2009) Multidetector CT of thoracic aortic aneurysms. Radiographics 29:537–552. doi:10.1148/rg.292075080

Arita T, Matsunaga N, Takano K et al (1997) Abdominal aortic aneurysm: rupture associated with the high-attenuating crescent sign. Radiology 204:765–768

Aronberg DJ, Glazer HS, Madsen K, Sagel SS (1984) Normal thoracic aortic diameters by computed tomography. J Comput Assist Tomogr 8:247–250

Azizi L, Henon A, Belkacem A et al (2004) Infected aortic aneurysms: CT features. Abdom Imaging 29:716–720

Bendel EC, Maleszewski JJ, Araoz PA (2011) Imaging sarcomas of the great vessels and heart. Semin Ultrasound CT MR 32:377–404

Bickerstaff LK, Pairolero PC, Hollier LH et al (1982) Thoracic aortic aneurysms: a population-based study. Surgery 92:1103–1108

Bruzzi JF, Remy-Jardin M, Delhaye D et al (2006) Multidetector row CT of hemoptysis. Radiographics 26:3–22. doi:10.1148/rg.261045726

Chiu KWH, Lakshminarayan R, Ettles DF (2013) Acute aortic syndrome: CT findings. Clin Radiol 68:741–748. doi:10.1016/j.crad.2013.03.001

Cho Y, Suzuki S, Katogi T, Ueda T (2004) Esophageal perforation of aortic arch aneurysm treated free of mediastinitis without manipulating esophagus. Japanese J Thorac Cardiovasc Surg Off Publ Japanese Assoc Thorac Surg Nihon Kyōbu Geka Gakkai zasshi 52:314–317

Choukroun EM, Labrousse LM, Madonna FP, Deville C (2002) Mobile thrombus of the thoracic aorta: diagnosis and treatment in 9 cases. Ann Vasc Surg 16:714–722

Coblentz L, Sallee DS (1988) Aortobronchopulmonary complicating aortic diagnosis in four cases fistula aneurysm. Ann Surg 150:535–538

Crass JR, Cohen AM, Motta AO et al (1990) A proposed new mechanism of traumatic aortic rupture: the osseous pinch. Radiology 176:645–649

Creasy JD, Chiles C, Routh WD, Dyer RB (1997) Overview of traumatic injury of the thoracic aorta. Radiographics 17:27–45. doi:10.1148/radiographics.17.1.9017797

Czerny M, Eggebrecht H, Sodeck G et al (2014) New insights regarding the incidence, presentation and treatment options of aorto-oesophageal fistulation after thoracic endovascular aortic repair: the European Registry of Endovascular Aortic Repair Complications. Eur J Cardiothorac Surg 45:452–457

da Silva ES, Tozzi FL, Otochi JP et al (1999) Aortoesophageal fistula caused by aneurysm of the thoracic aorta: successful surgical treatment, case report, and literature review. J Vasc Surg 30: 1150–1157

Daimon M, Watanabe H, Abe Y et al (2008) Normal values of echocardiographic parameters in relation to age in a healthy Japanese population: the JAMP study. Circ J 72:1859–1866

De Backer J, Loeys B, Devos D et al (2006) A critical analysis of minor cardiovascular criteria in the diagnostic evaluation of patients with Marfan syndrome. Genet Med 8:401–408

Demeter SL, Cordasco EM (1980) Aortobronchial fistula: keys to successful management. Angiology 31:431–435

Dorweiler B (2001) Endovascular treatment of acute bleeding complications in traumatic aortic rupture and aortobronchial fistula. Eur J Cardiothorac Surg 19:739–745

Edwards JE (1948) Anomalies of the derivatives of the aortic arch system. Med Clin North Am 32:925–949

Fang M, Agha S, Lockridge L et al (2001) Medical management of a large aortic thrombus in a young woman with essential thrombocythemia. Mayo Clin Proc 76:427–431

Favre JP, Gournier JP, Adham M et al (1994) Aortobronchial fistula: report of three cases and review of the literature. Surgery 115:264–270

Fayad ZY, Semaan E, Fahoum B et al (2013) Aortic mural thrombus in the normal or minimally atherosclerotic aorta. Ann Vasc Surg 27:282–290

Fillinger MF, Marra SP, Raghavan ML, Kennedy FE (2003) Prediction of rupture risk in abdominal aortic aneurysm during observation: wall stress versus diameter. J Vasc Surg 37:724–732

Fishman EK, Ney DR, Heath DG et al (2006) Volume rendering versus maximum intensity projection in CT angiography: what works best, when, and why. Radiographics 26:905–922. doi:10.1148/rg.263055186

Fueglistaler P, Wolff T, Guerke L et al (2005) Endovascular stent graft for symptomatic mobile thrombus of the thoracic aorta. J Vasc Surg 42:781–783

Gagliardi JM, Batt M, Khodja RH, Le bas P (1988) Mural thrombus of the aorta. Ann Vasc Surg 2:201–204

Garrett HE, Ricks RK, Lewis JM et al (1965) Hemoptysis secondary to aortopulmonary fistula; a report of two cases of successful treatment by operation. J Thorac Cardiovasc Surg 49:588–593

Garzón G, Fernández-Velilla M, Martí M et al (2005) Endovascular stent-graft treatment of thoracic aortic disease. Radiographics 25(Suppl 1):S229–S244. doi:10.1148/rg.25si055513

Gaylis H (1958) Aortic thrombosis. Circulation XVII:941

Girardi LN, Coselli JS (1997) Inflammatory aneurysm of the ascending aorta and aortic arch. Ann Thorac Surg 64:251–253

Goldstein SA, Evangelista A, Abbara S et al (2015) Multimodality imaging of diseases of the thoracic aorta in adults: from the American Society of Echocardiography and the European Association of Cardiovascular Imaging. J Am Soc Echocardiogr 28:119–182. doi:10.1016/j.echo.2014.11.015

Gomes MN, Choyke PL (1992) Infected aortic aneurysms: CT diagnosis. J Cardiovasc Surg (Torino) 33:684–689

Gonsalves CF (1999) The hyperattenuating crescent sign. Radiology 211:37–38

Gornik HL, Creager MA (2008) Aortitis. Circulation 117:3039–3051

Gotway MB, Dawn SK (2003) Thoracic aorta imaging with multislice CT. Radiol Clin North Am 41: 521–543

Graeber GM, Farrell BG, Neville JF, Parker FB (1980) Successful diagnosis and management of fistulas between the aorta and the tracheobronchial tree. Ann Thorac Surg 29:555–561

Green E, Klein S (2007). Multidetector row CT angiography of thoracic aorta. In P. Boiselle and C. White (Eds.), New techniques in cardiothoracic imaging. New York, NY: Informa Healthcare pp 105–126

Greenhalgh R (2004) Comparison of endovascular aneurysm repair with open repair in patients with abdominal aortic aneurysm (EVAR trial 1), 30-day operative mortality results: randomised controlled trial. Lancet 364:843–848

Grollman JH (1989) The aortic diverticulum: a remnant of the partially involuted dorsal aortic root. Cardiovasc Intervent Radiol 12:14–17

Hagspiel KD, Turba UC, Bozlar U et al (2007) Diagnosis of aortoenteric fistulas with CT angiography. J Vasc Interv Radiol 18:497–504

Halliday KE, al-Kutoubi A (1996) Draped aorta: CT sign of contained leak of aortic aneurysms. Radiology 199:41–43. doi:10.1148/radiology.199.1.8633170

Hastreiter AR, D'Cruz IA, Cantez T et al (1966) Right-sided aorta. I. Occurrence of right aortic arch in various types of congenital heart disease. II. Right aortic arch, right descending aorta, and associated anomalies. Br Heart J 28:722–739

Hausmann D, Gulba D, Bargheer K et al (1992) Successful thrombolysis of an aortic-arch thrombus in a patient after mesenteric embolism. N Engl J Med 327:500–501

Heckstall RL, Hollander JE (1998) Aortoesophageal fistula: recognition and diagnosis in the emergency department. Ann Emerg Med 32:502–505

Heystraten FM, Rosenbusch G, Kingma LM, Lacquet LK (1986) Chronic posttraumatic aneurysm of the thoracic aorta: surgically correctable occult threat. AJR Am J Roentgenol 146:303–308

Hiratzka LF, Bakris GL, Beckman JA et al (2010) ACCF/AHA/AATS/ACR/ASA/SCA/SCAI/SIR/STS/SVM guidelines for the diagnosis and management of patients with thoracic aortic disease: executive summary a report of the American College of Cardiology Foundation/American Heart Association Task Force on Practice Guidelines, American Association for Thoracic Surgery, American College of Radiology, American Stroke Association, Society of Cardiovascular Anesthesiologists, Society for Cardiovascular Angiography and Interventions, Society of Interventional Radiology, Society of Thoracic Surgeons, and Society for Vascular Medicine. J Am Coll Cardiol 55:e27–e129

Hirose Y, Takamiya M (1998) Growth curve of ruptured aortic aneurysm. J Cardiovasc Surg (Torino) 39:9–13

Hollander JE, Quick G (1991) Aortoesophageal fistula: a comprehensive review of the literature. Am J Med 91:279–287

Hoshina K, Sho E, Sho M et al (2003) Wall shear stress and strain modulate experimental aneurysm cellularity. J Vasc Surg 37:1067–1074

Hsiao EI, Kirsch CM, Kagawa FT et al (2001) Utility of fiberoptic bronchoscopy before bronchial artery embolization for massive hemoptysis. AJR Am J Roentgenol 177:861–867

Hughes FM, Kavanagh D, Barry M et al (2007) Aortoenteric fistula: a diagnostic dilemma. Abdom Imaging 32:398–402

Isselbacher EM (2005) Thoracic and abdominal aortic aneurysms. Circulation 111:816–828

Javadpour H, O'Toole JJ, McEniff JN et al (2002) Traumatic aortic transection: evidence for the osseous pinch mechanism. Ann Thorac Surg 73:951–953

Kälsch H, Lehmann N, Möhlenkamp S et al (2013) Body-surface adjusted aortic reference diameters for improved identification of patients with thoracic aortic aneurysms: results from the population-based Heinz Nixdorf Recall study. Int J Cardiol 163:72–78

Karalis DG, Chandrasekaran K, Victor MF et al (1991) Recognition and embolic potential of intraaortic atherosclerotic debris. J Am Coll Cardiol 17:73–78

Katayama Y, Suzuki H, Mizutani T (2000) Aorto-bronchial fistula after implantation of a self-expanding bronchial stent in a patient with aortic dissection. Japanese J Thorac Cardiovasc Surg Off Publ Japanese Assoc Thorac Surg Nihon Kyōbu Geka Gakkai zasshi 48:73–75

Keefer CSMK (1934) The pulmonary and pleural complications of aortic aneurysms. Am Heart J 10:208

Ketai LH, Mohammed T-LH, Kirsch J et al (2014) ACR appropriateness criteria® hemoptysis. J Thorac Imaging 29:W19–W22. doi:10.1097/RTI.0000000000000084

Khawaja FI, Varindani MK (1987) Aortoesophageal fistula. Review of clinical, radiographic, and endoscopic features. J Clin Gastroenterol 9:342–344

Kieffer E, Chiche L, Gomes D (2003) Aortoesophageal fistula: value of in situ aortic allograft replacement. Ann Surg 238:283–290

Lande A, Berkmen YM (1976) Aortitis: pathologic, clinical and arteriographic review. Radiol Clin North Am 14:219–240

Laperche T, Laurian C, Roudaut R, Steg PG (1997) Mobile thromboses of the aortic arch without aortic debris : a transesophageal echocardiographic finding associated with unexplained arterial embolism. Circulation 96:288–294

Larici AR, Franchi P, Occhipinti M et al (2014) Diagnosis and management of hemoptysis. Diagnos Interv Radiol 20:299–309. doi:10.5152/dir.2014.13426

Lau LS, Blanchard DG, Hye RJ (1997) Diagnosis and management of patients with peripheral macroemboli from thoracic aortic pathology. Ann Vasc Surg 11:348–353

Lawrie GM, Earle N, De Bakey ME (1994) Evolution of surgical techniques for aneurysms of the descending thoracic aorta: twenty-nine years experience with 659 patients. J Card Surg 9:648–661

Lee W-K, Mossop PJ, Little AF et al (2008) Infected (mycotic) aneurysms: spectrum of imaging appearances and management. Radiographics 28:1853–1868. doi:10.1148/rg.287085054

Lee RY, Flaherty L, Khushalani NI et al (2010) Aortoesophageal fistula: a rare fatal case caused by esophageal malignancy. J Gastrointest Oncol 1:64–65

Lehmann JM, Shnaker A, Silverberg D et al (2001) Arterial thromboembolism from a distal aortic thrombus in a patient with Crohn's disease. Isr Med Assoc J 3:226–227

Léobon B, Roux D, Mugniot A et al (2002) Endovascular treatment of thoracic aortic fistulas. Ann Thorac Surg 74:247–249

Lesko N, Link K, Grainger R (1997) The thoracic aorta, 3rd edn. Churchill Livingstone, Edinburgh, pp 854–857

Liu S-F, Chen Y-C, Lin M-C, Kao C-L (2004) Thoracic aortic aneurysm with aortobronchial fistula: a thirteen-year experience. Heart Lung 33:119–123. doi:10.1016/j.hrtlng.2003.12.008

Lodi R, Rajagopalan B, Blamire AM et al (2004) Abnormal cardiac energetics in patients carrying the A3243G mtDNA mutation measured in vivo using phosphorus MR spectroscopy. Biochim Biophys Acta 1657:146–150. doi:10.1016/j.bbabio.2004.05.003

Low RN, Wall SD, Jeffrey RB et al (1990) Aortoenteric fistula and perigraft infection: evaluation with CT. Radiology 175:157–162

Macedo TA, Stanson AW, Oderich GS et al (2004) Infected aortic aneurysms: imaging findings. Radiology 231:250–257

Machleder HI, Takiff H, Lois JF, Holburt E (1986) Aortic mural thrombus: an occult source of arterial thromboembolism. J Vasc Surg 4:473–478

MacIntosh EL, Parrott JC, Unruh HW (1991) Fistulas between the aorta and tracheobronchial tree. Ann Thorac Surg 51:515–519

Marco De Lucas E, Sádaba P, Lastra García-Barón P et al (2004) Value of helical computed tomography in the management of upper esophageal foreign bodies. Acta Radiol 45:369–374

McGloughlin TM, Doyle BJ (2010) New approaches to abdominal aortic aneurysm rupture risk assessment: engineering insights with clinical gain. Arterioscler Thromb Vasc Biol 30:1687–1694

Mehard WB, Heiken JP, Sicard GA (1994) High-attenuating crescent in abdominal aortic aneurysm wall at CT: a sign of acute or impending rupture. Radiology 192:359–362

Michel J-B, Martin-Ventura J-L, Egido J et al (2011) Novel aspects of the pathogenesis of aneurysms of the abdominal aorta in humans. Cardiovasc Res 90:18–27

Milano A, De Carlo M, Mussi A et al (1999) Aortobronchial fistula after coarctation repair and blunt chest trauma. Ann Thorac Surg 67:539–541

Mohammadi S, Trahan S, Miro S, Dagenais F (2007) Images in cardiovascular medicine. Large free-floating intra-aortic thrombus. Circulation 116:e142–e143

Motwani M, Kidambi A, Herzog BA et al (2013) MR imaging of cardiac tumors and masses: a review of methods and clinical applications. Radiology 268:26–43

Mower WR, Quiñones WJ, Gambhir SS (1997) Effect of intraluminal thrombus on abdominal aortic aneurysm wall stress. J Vasc Surg 26:602–608

Nagpal P, Khandelwal A, Saboo SS et al (2015) Modern imaging techniques: applications in the management of acute aortic pathologies. Postgrad Med J 91:449–462. doi:10.1136/postgradmedj-2014-133178

Nandi P, Ong GB (1978) Foreign body in the oesophagus: review of 2394 cases. Br J Surg 65:5–9

Oderich GS, Panneton JM, Bower TC et al (2001) Infected aortic aneurysms: aggressive presentation, complicated early outcome, but durable results. J Vasc Surg 34:900–908

Okita Y, Yamanaka K, Okada K et al (2014) Strategies for the treatment of aorto-oesophageal fistula. Eur J Cardiothorac Surg 46:894–900

Oldham KT, Johansen K, Winterscheid L, Larson EB (1983) Remembrance of things past: aortobronchial fistula 15 years after thoracic aortic homograft. West J Med 139:225–228

Oppenheim C, Naggara O, Touzé E et al (2009) High-resolution MR imaging of the cervical arterial wall: what the radiologist needs to know. Radiographics 29:1413–1431

Perdue GD, Smith RB, Ansley JD, Costantino MJ (1980) Impending aortoenteric hemorrhage: the effect of early recognition on improved outcome. Ann Surg 192:237–243

Piccinelli M, Vergara C, Antiga L et al (2013) Impact of hemodynamics on lumen boundary displacements in abdominal aortic aneurysms by means of dynamic computed tomography and computational fluid dynamics. Biomech Model Mechanobiol 12: 1263–1276

Picichè M, De Paulis R, Fabbri A, Chiariello L (2003) Postoperative aortic fistulas into the airways: etiology, pathogenesis, presentation, diagnosis, and management. Ann Thorac Surg 75:1998–2006

Pillari G, Chang JB, Zito J et al (1988) Computed tomography of abdominal aortic aneurysm. An in vivo pathological report with a note on dynamic predictors. Arch Surg 123:727–732

Pinilla I, Bret M, Cuesta E et al (2006) Role of computed tomography and magnetic resonance imaging in aortobronchial fistula diagnosis following aortic coarctation reparative surgery. Report of two cases. J Cardiovasc Surg (Torino) 47:221–227

Posniak HV, Olson MC, Demos TC et al (1990) CT of thoracic aortic aneurysms. Radiographics 10: 839–855

Pousios D, Velissaris T, Duggan S, Tsang G (2009) Floating intra-aortic thrombus presenting as distal arterial embolism. Interact Cardiovasc Thorac Surg 9:532–534

Raghavan ML, Vorp DA, Federle MP et al (2000) Wall stress distribution on three-dimensionally reconstructed models of human abdominal aortic aneurysm. J Vasc Surg 31:760–769

Rajagopalan S, Sanz J, Ribeiro VG, Dellegrottaglie S (2007) CT angiography of the thoracic aorta with protocols. In D. Mukherjee and S. Rajagopalan (Eds.), CT and MR angiography of the peripheral circulation: practical approach with clinical protocols, London, England: Informa Healthcare pp 91–110

Rakita D, Newatia A, Hines JJ et al (2007) Spectrum of CT findings in rupture and impending rupture of abdominal aortic aneurysms. Radiographics 27:497–507. doi:10.1148/rg.272065026

Raman SP, Kamaya A, Federle M, Fishman EK (2013) Aortoenteric fistulas: spectrum of CT findings. Abdom Imaging 38:367–375. doi:10.1007/s00261-012-9873-7

Reber PU, Patel AG, Stauffer E et al (1999) Mural aortic thrombi: an important cause of peripheral embolization. J Vasc Surg 30:1084–1089

Restrepo CS, Ocazionez D, Suri R, Vargas D (2011) Aortitis: imaging spectrum of the infectious and inflammatory conditions of the aorta. Radiographics 31:435–451. doi:10.1148/rg.312105069

Revel MP, Fournier LS, Hennebicque AS et al (2002) Can CT replace bronchoscopy in the detection of the site and cause of bleeding in patients with large or massive hemoptysis? AJR Am J Roentgenol 179:1217–1224. doi:10.2214/ajr.179.5.1791217

Revest M, Decaux O, Cazalets C et al (2007) Thoracic infectious aortitis: microbiology, pathophysiology and treatment. La Rev médecine interne/fondée par la Société Natl Fr médecine interne 28:108–115

Riesenman PJ, Brooks JD, Farber MA (2009) Thoracic endovascular aortic repair of aortobronchial fistulas. J Vasc Surg 50:992–998. doi:10.1016/j.jvs.2009.03.001

Romero J, Husain SA, Kelesidis I et al (2013) Detection of left atrial appendage thrombus by cardiac computed tomography in patients with atrial fibrillation: a meta-analysis. Circ Cardiovasc Imaging 6:185–194

Rossi PJ, Desai TR, Skelly CL et al (2002) Paravisceral aortic thrombus as a source of peripheral embolization – report of three cases and review of the literature. J Vasc Surg 36:839–843

Russo V, Garattoni M, Buia F et al (2015) 128-slice CT angiography of the aorta without ECG-gating: efficacy of faster gantry rotation time and iterative reconstruction in terms of image quality and radiation dose. Eur Radiol. doi:10.1007/s00330-015-3848-3

Safi H, Estrera A, Sheinbaum R, Miller C (2012) Indications, techniques and results of open repair of ascending and transverse aortic arch aneurysms, 6th edn. Wiley-Blackwell, Oxford, UK

Sakalihasan N, Limet R, Defawe OD (2005) Abdominal aortic aneurysm. Lancet (London, England) 365:1577–1589

Seymour EQ (1978) Aortoesophageal fistula as a complication of aortic prosthetic graft. AJR Am J Roentgenol 131:160–161

Shapiro MD, Neilan TG, Jassal DS et al (2007) Multidetector computed tomography for the detection of left atrial appendage thrombus: a comparative study with transesophageal echocardiography. J Comput Assist Tomogr 31:905–909

Shuford WH, Sybers RG, Gordon IJ et al (1986) Circumflex retroesophageal right aortic arch simulating mediastinal tumor or dissecting aneurysm. AJR Am J Roentgenol 146:491–496

Siegel CL, Cohan RH, Korobkin M et al (1994) Abdominal aortic aneurysm morphology: CT features in patients with ruptured and nonruptured aneurysms. AJR Am J Roentgenol 163:1123–1129

Slobodin G, Naschitz JE, Zuckerman E et al (2006) Aortic involvement in rheumatic diseases. Clin Exp Rheumatol 24:S41–S47

Speelman L, Schurink GWH, Bosboom EMH et al (2010) The mechanical role of thrombus on the growth rate of an abdominal aortic aneurysm. J Vasc Surg 51:19–26

Sueyoshi E, Sakamoto I, Kawahara Y et al (1998) Infected abdominal aortic aneurysm: early CT findings. Abdom Imaging 23:645–648

Svensson LG, Crawford ES, Hess KR et al (1993) Experience with 1509 patients undergoing thoracoabdominal aortic operations. J Vasc Surg 17:357–368; discussion 368–370

Task A, Erbel R, Germany C et al (2014) 2014 ESC Guidelines on the diagnosis and treatment of aortic diseases. Eur Heart J 35:2873–2926. doi:10.1093/eurheartj/ehu281

Thalheimer A, Fein M, Geissinger E, Franke S (2004) Intimal angiosarcoma of the aorta: report of a case and review of the literature. J Vasc Surg 40:548–553

Ting AC, Cheng SW (1997) Femoral pseudoaneurysms in drug addicts. World J Surg 21:783–786; discussion 786–787

Tsao JW, Marder SR, Goldstone J, Bloom AI (2002) Presentation, diagnosis, and management of arterial mycotic pseudoaneurysms in injection drug users. Ann Vasc Surg 16:652–662

Tsilimparis N, Hanack U, Pisimisis G et al (2011) Thrombus in the non-aneurysmal, non-atherosclerotic descending thoracic aorta – an unusual source of arterial embolism. Eur J Vasc Endovasc Surg 41:450–457

Tunick PA, Culliford AT, Lamparello PJ, Kronzon I (1991) Atheromatosis of the aortic arch as an occult source of multiple systemic emboli. Ann Intern Med 114:391–392

Uittenbogaart M, Sosef MN, van Bastelaar J (2014) Sentinel bleeding as a sign of gastroaortic fistula formation after oesophageal surgery. Case Rep Surg 2014:614312

Upchurch G (2014) Thoracic and Thoracoabdominal Aortic Aneurysms. In J. Cronenwett and K. Johnston (Eds.). Rutherford's vascular surgery. Philadelfia, Pennsylvania, USA: Elsevier. 8th ed., pp 2084–2101

Vasan RS, Larson MG, Levy D (1995) Determinants of echocardiographic aortic root size. The Framingham Heart Study. Circulation 91:734–740

Verbeeck N, Cavez N, Plawny L et al (2014) Primary aortic thrombosis : role of enhanced multislice CT demonstrated in three exceptional cases. JBR-BTR J Belge Radiol 97:76–80

Verma H, Meda N, Vora S et al (2014) Contemporary management of symptomatic primary aortic mural thrombus. J Vasc Surg 60:1524–1534. doi:10.1016/j.jvs.2014.08.057

Vernhet H, Serfaty JM, Serhal M et al (2004) Abdominal CT angiography before surgery as a predictor of postoperative death in acute aortic dissection. AJR Am J Roentgenol 182:875–879

Vogelzang RL, Sohaey R (1988) Infected aortic aneurysms: CT appearance. J Comput Assist Tomogr 12:109–112

von Falck C, Meyer B, Fegbeutel C et al (2013) Imaging features of primary Sarcomas of the great vessels in CT, MRI and PET/CT: a single-center experience. BMC Med Imaging 13:25. doi:10.1186/1471-2342-13-25

von Segesser L (1997) Aortobronchial and aortoesophageal fistulae as risk factors in surgery of descending thoracic aortic aneurysms. Eur J Cardiothorac Surg 12:195–201

Vu QDM, Menias CO, Bhalla S et al (2009) Aortoenteric fistulas: CT features and potential mimics. Radiographics 29:197–209

Wei Y, Chen L, Wang Y et al (2015) Proposed management protocol for ingested esophageal foreign body and aortoesophageal fistula: a single-center experience. Int J Clin Exp Med 8:607–615

Weininger M, Barraza JM, Kemper CA et al (2011) Cardiothoracic CT angiography: current contrast medium delivery strategies. Am J Roentgenol 196:W260–W272. doi:10.2214/AJR.10.5814

Wolak A, Gransar H, Thomson LEJ et al (2008) Aortic size assessment by noncontrast cardiac computed tomography: normal limits by age, gender, and body surface area. JACC Cardiovasc Imaging 1:200–209

Yasuda F, Shimono T, Tonouchi H et al (2002) Successful repair of an aortoesophageal fistula with aneurysm from esophageal diverticulum. Ann Thorac Surg 73:637–639

Yeo DL, Haider S, Alexandra C, Zhen C (2015) Blunt traumatic aortic injury of right aortic arch in a patient with an aberrant left subclavian artery. Yale J Biol Med 88:93–97